Synthesis, luminescent properties and application opportunities of C-substituted *ortho*-carborane π-conjugated luminophores: a mini review

Timofey D. Moseev [a] *, Tair A. Idrisov [a], Mikhail V. Varaksin [ab] *, Valery N. Charushin [ab], Oleg N. Chupakhin [ab]

a: Institute of Chemical Engineering, Ural Federal University, Ekaterinburg 620062, Russia
b: I.Ya. Postovsky Institute of Organic Synthesis, Ural Branch of the RAS, Ekaterinburg 620066, Russia
* Corresponding authors: timofey.moseev@urfu.ru, m.v.varaksin@urfu.ru

Abstract

The mini-review summarizes the recent achievements in the synthesis of C-substituted *ortho*-carborane luminophores bearing an alkenyl- or alkynyl- π-conjugated system. The luminescence properties, such as absorbance, emission peaks, photophysical effects (particularly intramolecular charge transfer), local excitation, dual emission, and structure-property relationships are comprehensively studied. The advantages of the diverse applications for this type of *o*-carborane cluster compounds as organic light-emitting diodes (OLEDs), semiconductors, chemosensors, and other components of modern organic electronics are extensively discussed. In addition, the existing limitations in the chemical design and application possibilities are also considered.

Key findings

● The synthesis and properties of *ortho*-carborane-derived luminophores containing a multiple bond conjugated system are considered.

● The photophysical properties of the C-substituted *ortho*-carborane π-conjugated compounds and the devices fabricated on them are discussed.

● The review contains 82 references and covers known data from 2009 to the present.

1. Introduction

Carboranes are compounds having several carbon and boron atoms located at the vertices of convex polyhedra with triangular faces as the basic structural unit [1–2]. The formation of three-centered two-electron bonds is characteristic of boron atoms in such structures, which determines the cluster structure and delocalization of electron density (σ-aromaticity) of carboranes [3–4]. In *closo*-carboranes, the number of carbon and boron atoms is equal to the number of vertices of a convex polyhedron with triangular faces; in *nido*-carboranes the number of carbon and boron atoms is one less than the number of vertices of a convex polyhedron with triangular faces, and in *arachno*-carboranes it is two less (Figure 1).

The most stable and synthetically available among carboranes are dicarba-*closo*-dodecaboranes compounds with the formula $C_2B_{10}H_{12}$, C- and B-atoms of which form an icosahedral polyhedron (convex twenty-sided polyhedron with triangular faces).

According to the position of C-atoms in the polyhedron, 1,2-dicarba-*closo*-dodecaborane (*ortho*-carborane, *o*-carborane), 1,7-dicarba-*closo*-dodecaborane (*m*-carborane), and 1,12-dicarba-*closo*-dodecaborane (*p*-carborane) are distinguished. It is worth noting that in the *o*-carborane cluster the C-H bonds, unlike the B-H bonds, are strongly polarized (in the *m*- and *p*-isomers the polarization is less) because of electron density delocalization. Electron delocalization also causes a strong negative inductive effect (-I) of the *o*-carboranyl substituent in C-substituted *o*-carborane derivatives [5].
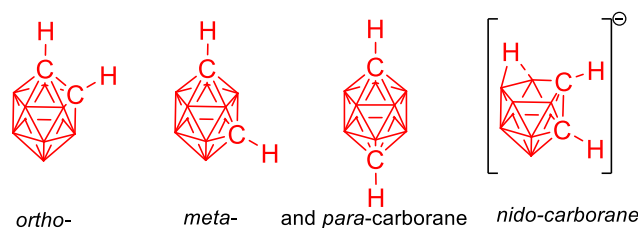
Figure 1 The structure of *ortho*-, *meta*-, *para*-, and *nido*-carborane.

Advanced materials based on *o*-carborane have been widely used in the field of molecular electronics and related fields due to their synthetic availability and wide functionalization possibilities. For example, they can be used as organic light-emitting diodes (OLEDs), field-effect transistors (FETs), molecular rectifiers, photovoltaic converters (PV cells), optical- or chemosensors, photosensitizers, and catalysts (Figure 2) [6–9].

The design of π-conjugated systems with *o*-carboranyl fragments is an advanced strategy in the oriented synthesis of functional optical materials, since the incorporation of boronyl clusters makes it possible to control the molecular architecture of these materials and intramolecular electronic effects, and also imparts thermal, electrochemical, and photostability. Due to the highly-organized structure of the carboranyl moiety in such photoactive systems, emission often occurs not only in solutions, but also in crystals and aggregates [10–11]. Most molecules of organic luminophores consist of conjugated π-systems and/or transition metal complexes. A rather effective strategy for narrowing the energy gap between HOMO and LUMO (forbidden band width) and thus shifting absorption and emission to the long-wavelength region is to expand the π-conjugation system by one multiple bonds. The simultaneous involvement of electron-donating and electron-withdrawing group (EDG and EWG, respectively) in the π-conjugation is known as push-pull systems, namely D-π-A, A-π-D-π-A, D-π-A-π-D, etc., where D is an EDG, π is a π-linker, and A is an EWG, which might reduce the energy difference between HOMO and LUMO even more significantly [12–15]. Double (alkenyl) or triple (alkynyl) bonds can be used as π-linkers to control and change the degree of rotation and oscillation of individual fragments relative to each other, which directly affects the optical properties in solutions and solid states. For example, ethenyl moieties cause free rotation relative to the double bond axis of both the carboranyl and aromatic moiety, which can lead to TICT (twisted intramolecular charge transfer) or different emission of cis/trans isomers. On the contrary, the ethynyl linker, because of its linear structure, does not allow the fragments to rotate relative to each other, but the rotation of *o*-carborane is still possible; thus, a more ordered packing of molecules in crystals can be achieved [16-18]. In addition, the spatial separation of chromophore groups favors the formation of excimer and exciplex. In general, EDG might be various hetero- and polyaromatic derivatives, and by changing these substituents one can achieve the desired values of quantum yield, emission and absorption wavelengths, etc. [19-20]. Besides using a carboranyl cluster as EWG, one is the most diverse groups in push-pull system are those resulting from single group (e.g., cyan, carboxyl, etc.), heterocycles (e.g., triazines or imidazole and other azines and azoles), fluoroaromatics and other [21–27].
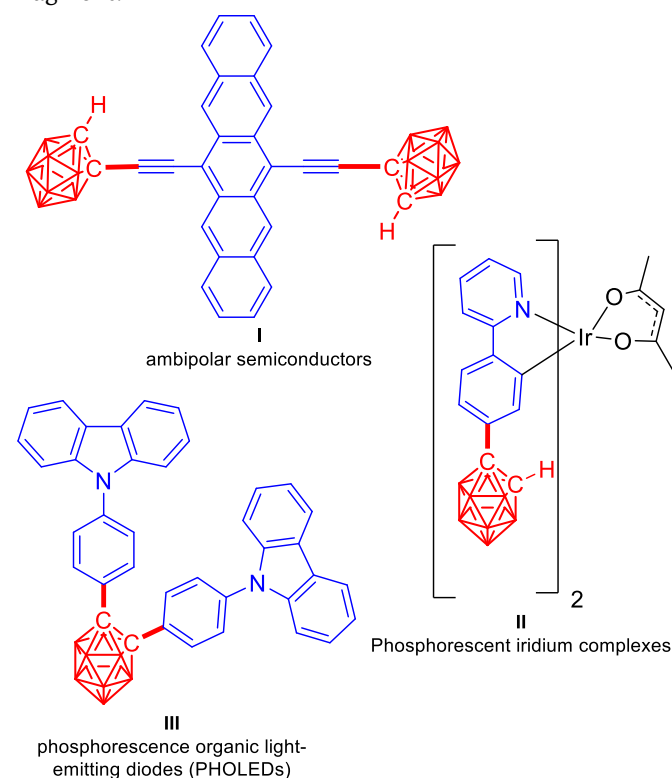
Thus, the unique spatial and electronic structure of such finely tuned *o*-carboranyl systems determines their technologically relevant luminescent properties as well as application possibilities in the design of materials for organic molecular electronics, bioimaging, and other promising areas of science. For the synthesis of these molecules, the two synthetic approaches can be distinguished. In the first one, the *o*-carborane cluster is formed by cycloaddition of decaborane(14) with alkynes (decaborane strategy); in this case a π-conjugated system is already present in the molecule or additional modification is necessary to obtain it. The second strategy involves the use of *o*-carboranyl synthons in which the multiple bonds are directly bonded to the *o*-carborane or *via* an aromatic or aliphatic spacer (Figure 3).

There are several reviews in the literature on luminescent materials based on *o*-carboranyl derivatives, but there is no analytical review on conjugated carboranyl fragments [28–36]. Thus, this paper deals with the classification of known methods and approaches for the preparation of alkynyl and alkenyl π-conjugated *o*-carboranyl systems, discussion of their optical properties, and their potential applications in molecular electronics and related fields.

2. Luminophores based on alkenyl π-conjugated systems

Luminophores based on alkenyl derivatives of *o*-carborane are not widely reported in the literature, with just over ten different works in this field currently known. The most common object on which scientists design photoactive systems is a styrene fragment that is directly or through a methylene moiety bonded to the *o*-carborane fragment.

I
ambipolar semiconductors

II
Phosphorescent iridium complexes

III
phosphorescence organic light-emitting diodes (PHOLEDs)

**Figure 2** Advanced materials of organic electronics based on *ortho*-carborane.

Key organic frameworks considered in this review
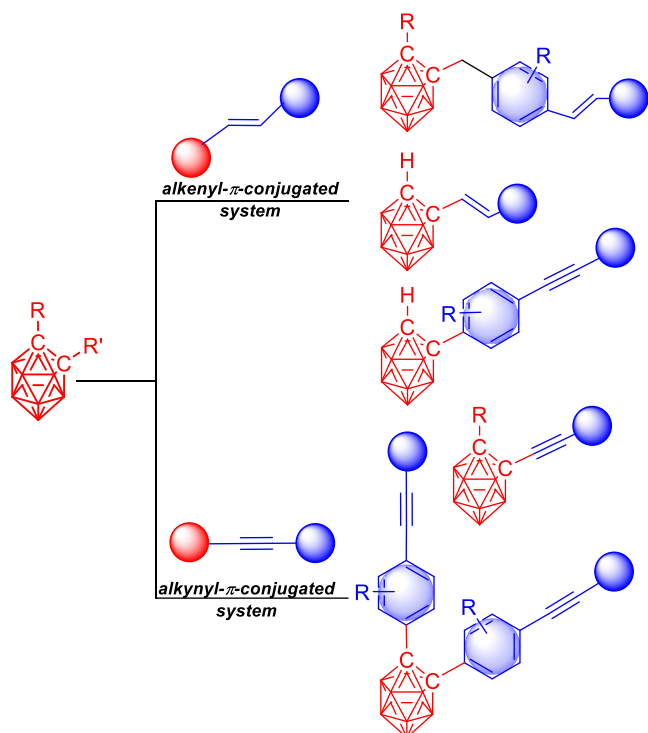
Figure 3 Alkenyl and alkynyl π-conjugated systems based on *o*-carboranyl derivatives.

In almost all examples, the synthetic strategy for obtaining such structures consists of two steps, the first of which consist of functionalization of the *o*-carborane cluster, and the next involves modification of this molecule to obtain the target photoactive systems.

R. Núñez et al. in 2012 for the first time synthesized a series of *o*-carboranyl fluorophores containing a styrenyl moiety [37]. To obtain desired molecules, *o*-carborane was first lithiated in dry THF and then coupled with 4-vinylbenzyl chloride (VBC) leading to mono- and disubstituted **2a–d** derivatives in 40–76% yields (Scheme 1). Anionic compounds **3a–d** with tetra-methylammonium as cation were further synthesized from the same compounds. Both types of fluorophores have similar properties, with absorption spectra showing a maximum in the region of 254 nm and another band with a small intensity around 295 nm. Emission was detected in the blue region with a maximum around 312 nm; the exception was compound **2b** with a band at 409 nm (Figure 4 and 5). Quantum yields for the closo-*o*-carboranyl fluorophores reached 40% and 20% for **2a** and **2c**, while they did not exceed 2% for the *nido*-derivatives. The authors also found that **2b**, containing a phenyl substituent at the C(2)-carbon atom, are an example of a D-A-type push-pull system in which the EDG is styrene and the C-substituted *o*-carborane acts as an EWG. Such photophysical properties were most likely due to the presence of a spacer (–CH$_2$–) between the two functional fragments of the system. A few years later, the authors proved by computational methods that the use of *m*-derivatives instead of *o*-carboranyl does not affect the absorption and emission properties [38]. In addition, the hypothesis about the negative influence of the methylene group on the luminescent properties was also confirmed.
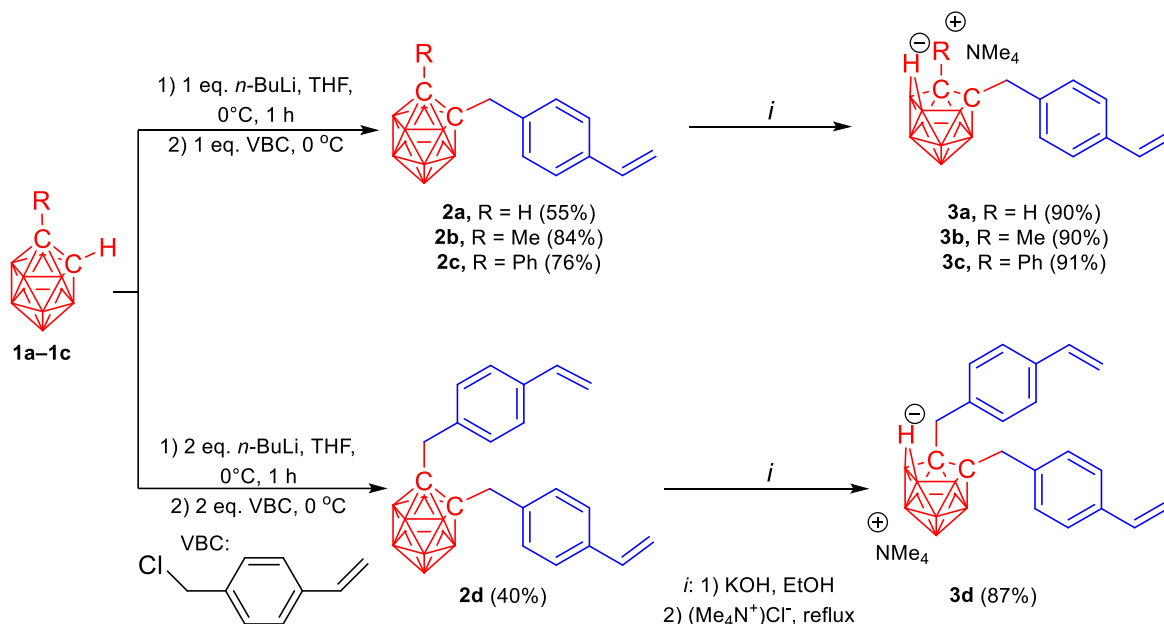
Scheme 1 Synthesis of *closo-* and *nido-*styrene-containing *o*-carborane derivatives.
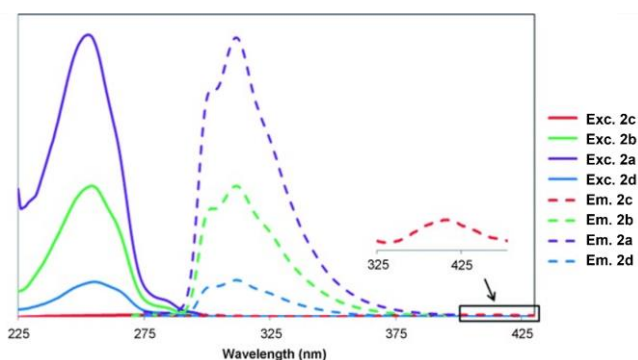
Figure 4 Normalized excitation and emission spectra of **2a–d** in acetonitrile. Reproduced from R. Núñez and co-workers [37] with permission from the Wiley.
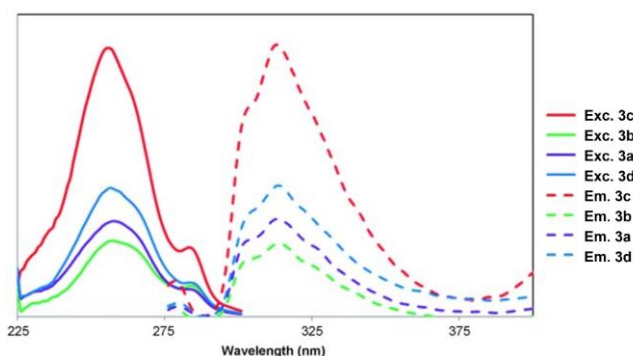
Figure 5 Normalized excitation and emission spectra of **3a–d** in acetonitrile. Reproduced from R. Núñez and co-workers [37] with permission from the Wiley.

In their next work, R. Núñez et al. continued [39] the functionalization of the previously obtained styrene derivatives of *o*-carborane. A Pd-catalyzed Heck reaction with aryl iodides was used to increase the conjugation system, and a series of molecules **4a–c** were obtained in 75–88% yields, including (bis)carboranyl derivatives **5a–b** in 78–88% yields (Scheme 2). It is worth noting that analogous *m*-carboranyl derivatives with similar yields were also synthesized in this work. Compared to the previously obtained compounds (Scheme 1), the novel fluorophores possessed longer absorption (315–320 vs. 255 nm) and emission (350–370 vs. 312 nm) wave-

lengths, as well as approximately 1.5 times larger values of the molar absorption coefficient. The authors suggested that the carborane cluster interferes with π–π interactions and reduced intramolecular rotation, which led to a bathochromic shift in emission. Consequently, the quantum yields were smaller and did not exceed 16%, but for the *m*-carboranyl derivatives they reached 19% in some cases. In addition, the presence of emission in powder and thin films for compound **5b** was discovered for the first time with the appearance of a new band in the green region 520–540 nm. Most likely, these properties were due to the formation of aggregates, which was further confirmed by experiments in aqueous solutions (Figure 6).

Taking into account the promising photophysical properties of carboranyl-stilbene dyads, R. Núñez et al. synthesized [40–41] molecules with extended π-conjugation system based on different aryls (phenyl, biphenyl, anthracene and tetraphenylethylene) in several works (Scheme 3).

The only difference in the synthetic procedure was the use of aryl bromides instead of iodides, most likely due to better commercial availability; the yields remained at the similar range of 40–76%. Quite expectedly, a bathochromic shift in emission and absorption was observed as the conjugated system was extended, along with an increase in molar extinction coefficients of up to 80 000.

Compounds **6a** and **7a** had absorbance in the 355–362 nm region and emitted blue light at 418–425 nm, and twice as high quantum yields were recorded, reaching 47%. Anthracene derivative and its *m*-carboranyl analog had yellow-orange luminescence in the region of 560 nm; however, QY did not exceed 7%. The authors attributed this to the quenching of fluorescence because of rotation around the double bond. In this case, the *o*-carboranyl substituent did not prevent the non-radiative relaxation due to the large energy barrier of the rotation. All compounds showed the ability to form aggregates with a bathochromic shift of about 40 nm for **6a** and **7a** and hypsochromic (15 nm) for **8a**.
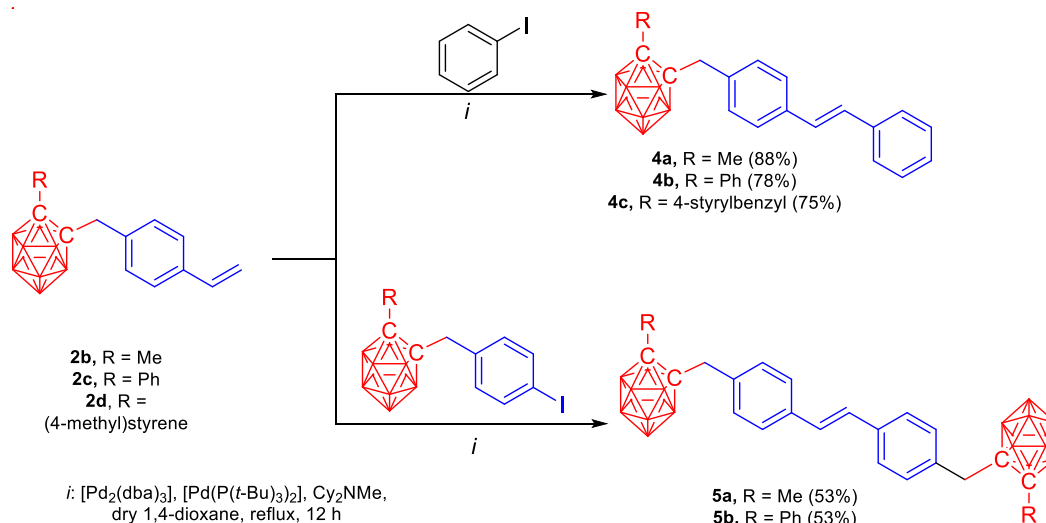
**Scheme 2** Synthesis of *o*-carboranyl-stilbene dyads.
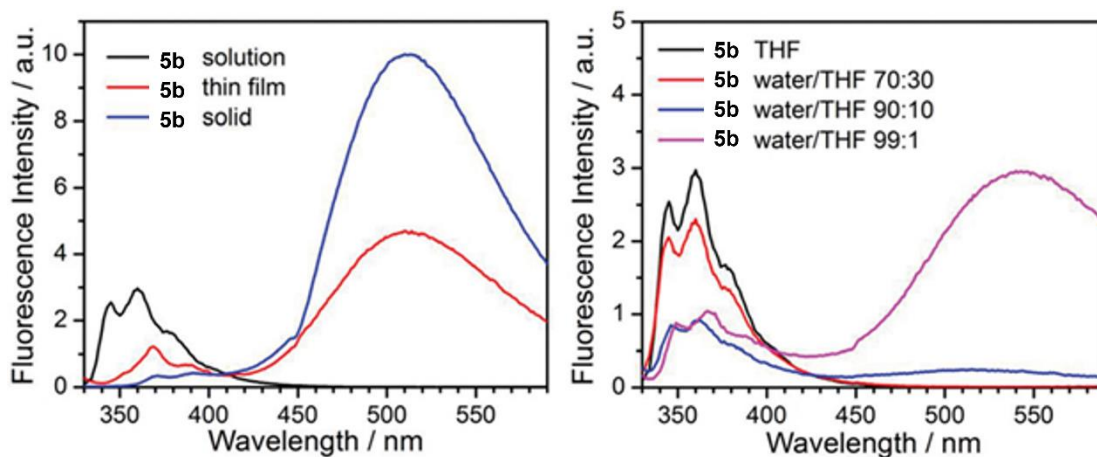
Figure 6 Emission spectra of **5b** in solution (THF), solid and thin film at λ_{ex} = 310 nm (left). Emission spectra of **5b** at different THF:H$_2$O ratios at λ_{ex} = 320 nm (right). Reproduced from R. Núñez and co-workers [39] with permission from the Royal Society of Chemistry.

It is worth mentioning that the tetraphenylethylene derivative possessed emission in the yellow region at 560 nm with QY of up to 12%. However, when aggregates were formed, the quantum yields increased significantly to 56%, with no emission changes being observed. The authors attributed this result to the absence of exciton interactions (Figure 7).

Over the last few decades, BODIPY fluorophores found applications as organic light-emitting diodes and semiconductors. Of particular note is their application as molecules for bioimaging; due to their long wavelength emission, they were capable of reaching the biological window [42]. R. Núñez and C. Prandi et al. [43] modified this class of fluorophores and its aza-analog (aza-BODIPY) with a fragment of *o*- and *m*-carborane and demonstrated their utilization for visualization of cellular structures (Scheme 4). The authors used a Heck cross-coupling to synthesize the target derivatives **12–13** in 46–60% yields. It is worth noting that BODIPY derivative **12** exhibited green emission in the 512 nm region with a quantum yield of 40%, while its aza analog **13a** emitted photons in the red region of 705 nm with a quantum yield of less than 1.5%. The authors explained this result by the reason that **13a** has a more developed π-conjugation system compared to **12**. The non-functionalized molecules (*meso*-phenyl-1,3,5,7-tetramethyl-BODIPY, tetraphenyl-aza-BODIPY, *meso*-phenyl-3,5-dithienyl-BODIPY) had a similar emission pattern but higher quantum yields of 56, 1.9, 84%, respectively. Thus, the incorporation of a carboranyl moiety into BODIPY fluorophores led to a significant decrease in fluorescence efficiency. It is worth noting that no significant difference in photophysical properties was found for *m*-carboranyl derivatives compared to *o*-derivatives.

The modification of BODIPY fluorophores continued with the preparation of 2,6- and 3,5-distyrenyl-substituted *o*-carbonyl derivatives **15**. It is worth noting that in this work R. Núñez and C. Prandi et al. [44] focused their attention on obtaining *m*-carboranyl derivatives, and the *o*-carboranyl fragment is represented by only one example

(Scheme 5). The authors employed a similar synthetic strategy to derive the target molecules in 30–55% yields. All obtained compounds demonstrated almost the same photophysical properties with absorption in the 550–570 nm region and emission in the of 633–651 nm; the quantum yields were of 5 to 12% (Figure 8). It is remarkable that the 3,6-nonfunctionalized carboranyl fragment derivative (meso-phenyl-3,5-distyryl-BODIPY) had a QY as high as 83%, while meso-phenyl-2,6-distyryl-BODIPY had a QY equal to 1%. Thus, the incorporation of the *o*-carborane cluster at the C(2) and C(6) positions of BODIPY improved the spectral characteristics, while the modification at the C(3) and C(5) positions led to their deterioration. As in the previous work, no significant difference between *ortho*- and *m*-carboranyl derivatives in photophysical properties was found.
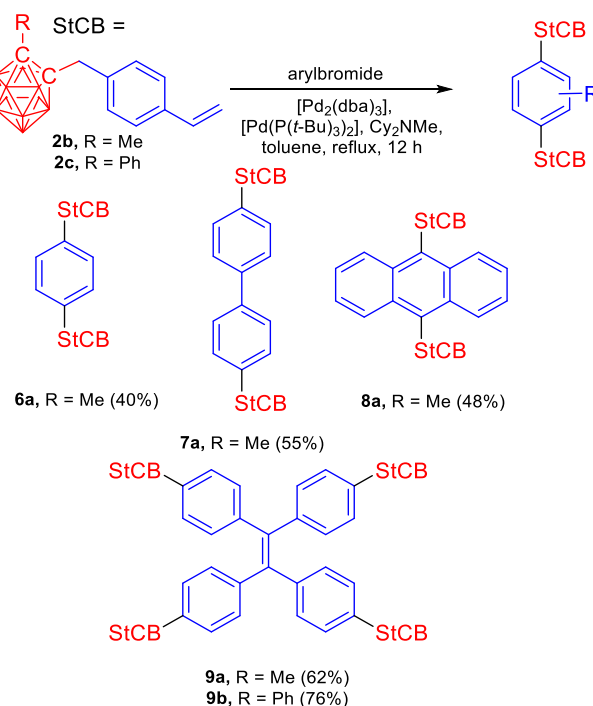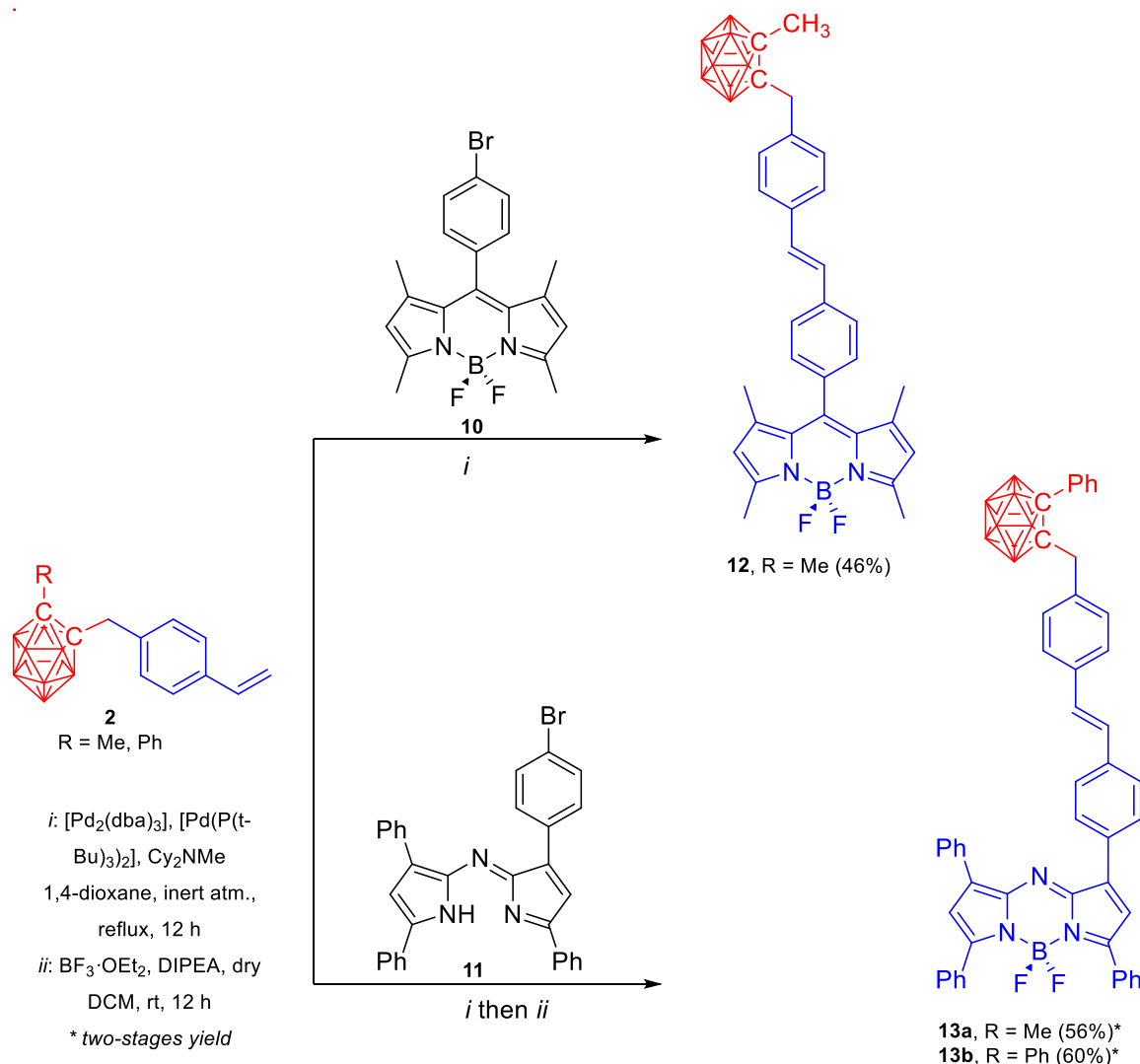

Scheme 3 Synthesis of *o*-carboranyl-containing distyryl aromatic carborane systems.
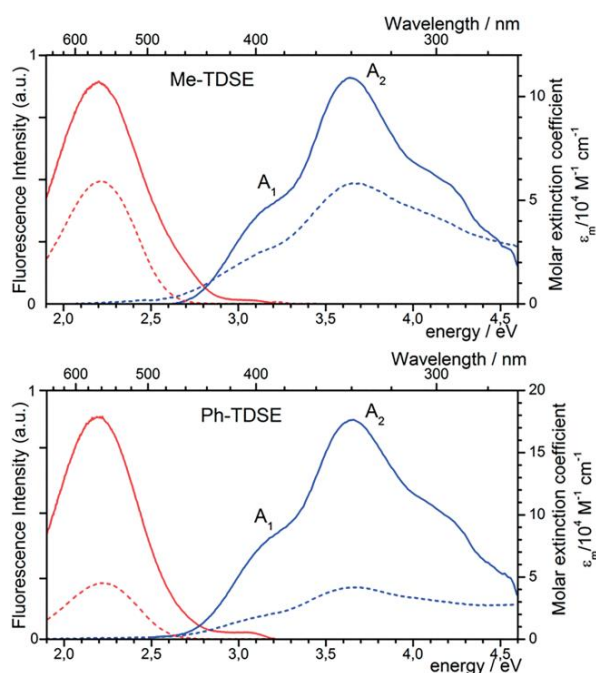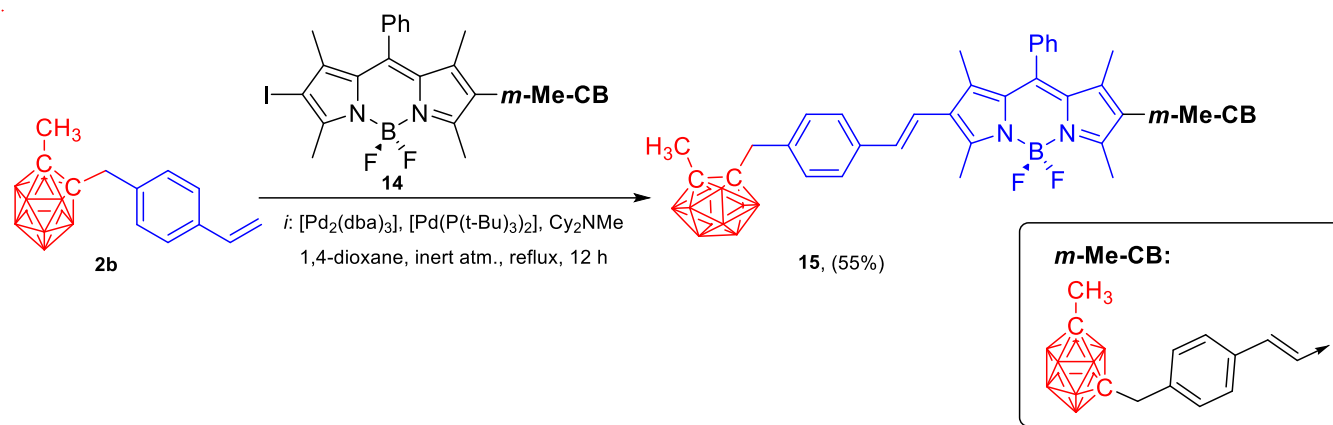
Figure 7 Absorption and emission spectra (left) of **9a** (top) and **9b** (bottom) in THF (solid lines) and THF/H$_2$O (1:1000, v/v; dotted lines). Reproduced from R. Núñez and co-workers [40] with permission from the Wiley.

One more example of BODIPY fluorophores [45] containing alkenyl π-conjugated system is triads of *o*-carborane, dipyrrolylmethane and tetraphenylethylene (Scheme 6). I. Nar and A. Atsay et al. suggested a procedure for the synthesis from ethynyl derivative of BODIPY in two steps. In the first step, Sonogashira reaction with aryl bromide was employed. The subsequent condensation with decaborane(14) led to the target compound in an overall yield of 25%. The obtained fluorophore exhibited two absorption bands at 311 and 502 nm, the first most likely associated with the absorption of the tetraphenylethylene moiety and the second related to the absorption of BODIPY. One band in the emission spectra was detected in the 513 nm region, which could be attributed to the local excitation (LE) state. Some examples have been reported in the literature and in this review where the incorporation of a carboranyl moiety resulted in a reduction of aggregation-caused quenching (ACQ, aggregation-caused quenching) because of a decrease in π-π stacking. However, in this case, the modification by the BODIPY fluorophore of the *o*-carboranyl fragments did not lead to a decrease in the ACQ properties.
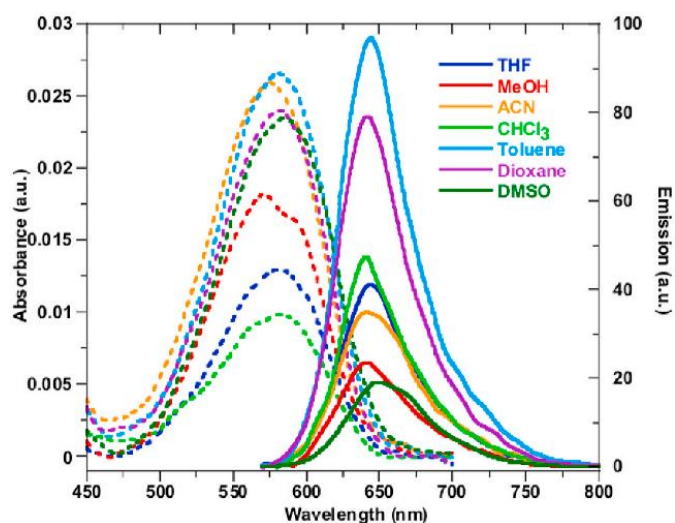

Scheme 4 Synthesis of *o*-carboranyl-containing BODIPY and aza-BODIPY.

Scheme 5 Synthesis of 2,6-substituted *o*-carboranyl-containing BODIPYs.
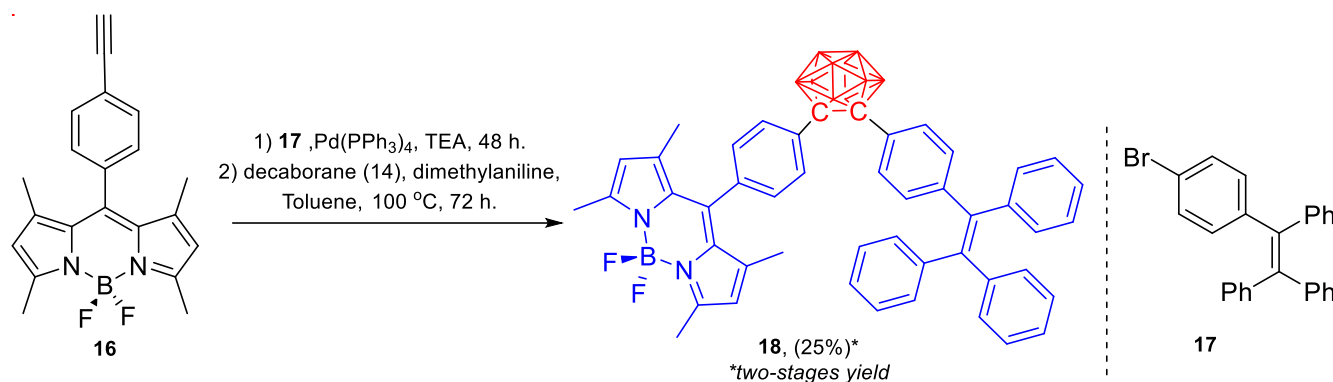
Scheme 6 Synthesis of the triad of *o*-carborane, dipyrrolylmethane and tetraphenylethylene.


Figure 8 Absorption and emission spectra **15**. Reproduced from R. Núñez and co-workers [44] with permission from the Elseiver.

Octasilsesquioxanes (T8 or OVC) are three-dimensional organosilicate compounds with the general formula [RSiO$_{1.5}$]$_8$, which are characterized by high thermal stability and can be readily synthesized. R. Núñez et al. [46] suggested a way to modify this framework with **19** *o*-carboranyl moieties. The Heck reaction yielded novel supramolecular compounds **20a-c** in 43–62% yields, and a *m*-carboranyl analog was also synthesized (Scheme 7). For all the obtained compounds, similar spectral characteristics were observed with an absorption maximum at 338 nm and emission at 391 nm (Figure 9). The quantum yield

of unsubstituted *o*-carborane (R = H) was almost twice (59%) higher than that of the series of substituted analogs (R = Me, Ph). The authors explained this result by the fact that the modification of the second C-atom of *o*-carborane increased the degree of non-radiative transitions (k_{NR}) as a result of steric hindrances and intramolecular repulsions of fragments. This hypothesis was supported considering that the quantum yields in the films for all compounds were around 6–7% and the k_{NR} constants are in the range of 0.82–1.0 ns^{-1}. It is worth noting that the compound (*p*-methyl-stilbene-vinyl)$_8$OVS) without the *o*-carboranyl fragments had a QY of 22%; therefore, the incorporation of the *o*-carboranyl moiety leads to a significant enhancement of the luminescence efficiency. As in all previous cases, no significant difference in luminescence properties was found compared to the *m*-carboranyl derivative.

Fluorene [47] is a polycyclic aromatic hydrocarbon, on the basis of which photoactive systems with a variety of properties could be designed. R. Núñez and A. Sousa-Pedrares et al. [46] proposed a method for the synthesis of fluorene-*o*-carboranyl systems, in which the two fragments were bonded to each other directly or through a silyl spacer (Scheme 8). To synthesized the former, first condensation with decaborane(14) was carried out, and then intermediate was modified with vinylbenzyl chloride (VBS) to give **22**. A further Pt-catalyzed reaction of **21b** with **23a–b** was employed to obtain fluorophores in which the carboranyl substituent was distanced from the fluorene substituent.
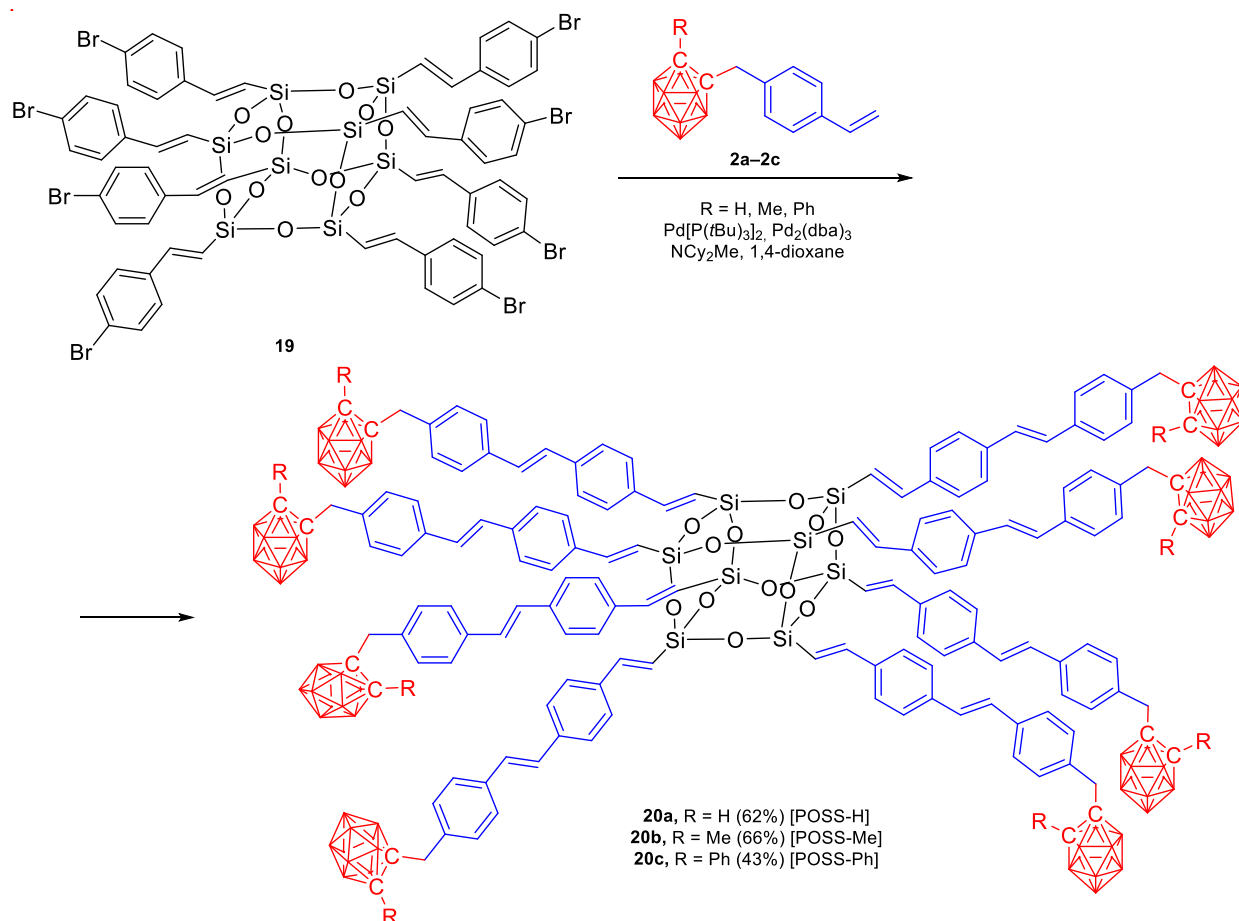
Scheme 7 Synthesis of octasylsesquioxanes functionalized with *o*-carboranyl-containing vinylstilbene.
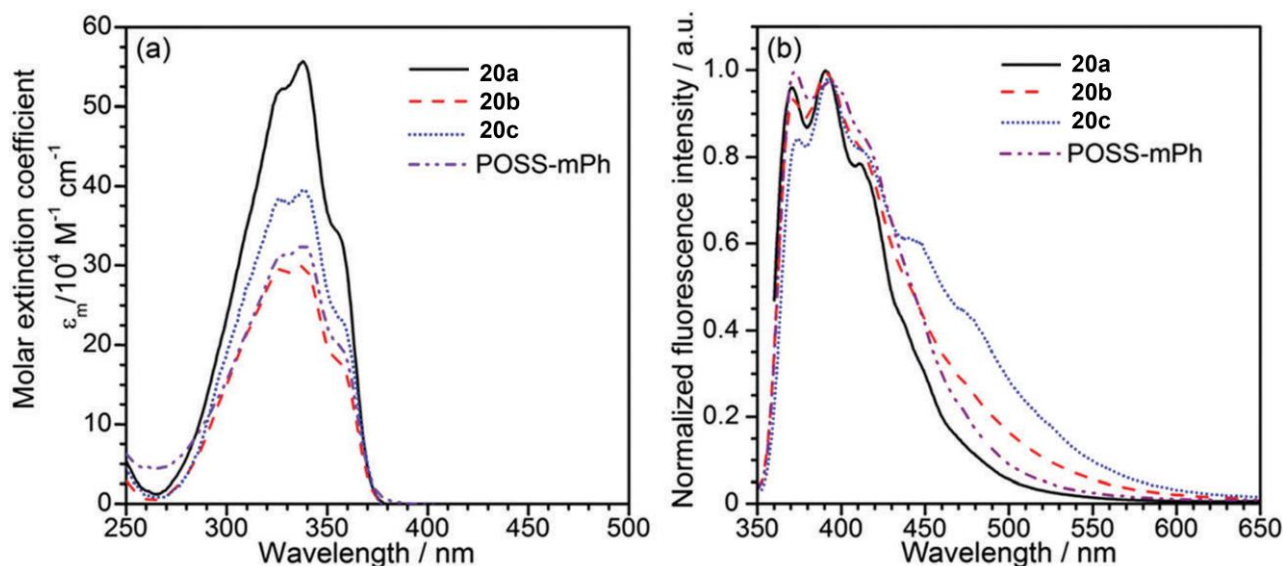
Figure 9 Absorbance (left) and emission (right) spectra of **25a–c** and the *m*-carboranyl analogue (POSS-mPh). Reproduced from R. Núñez and co-workers [46] with permission from the Royal Society of Chemistry.

As a result, a series of novel photoactive compounds were obtained in 55–78% yields. The synthesized fluorophores possessed three-four absorption bands in the near-UV region of 259–315 nm and violet emission in the 350 nm region. It is worth noting that **24–25**, in which the *o*-carboranyl substituent was located away from the fluorene, show a QY of 27–37%. The authors hypothesized that in the presence of the spacer the fluorene acted as an EDG and the *o*-carborane was the EWG. In compound **20**, where the carboranyl-fluorene system was a strong EWG and the styrenyl fragment was a weak EDG, the PET (photoinduced electron transfer) process results in quenching of the emission. Thus, photoluminescent properties could be improved by using spacers to separate the different photoactive moieties relative to each other.
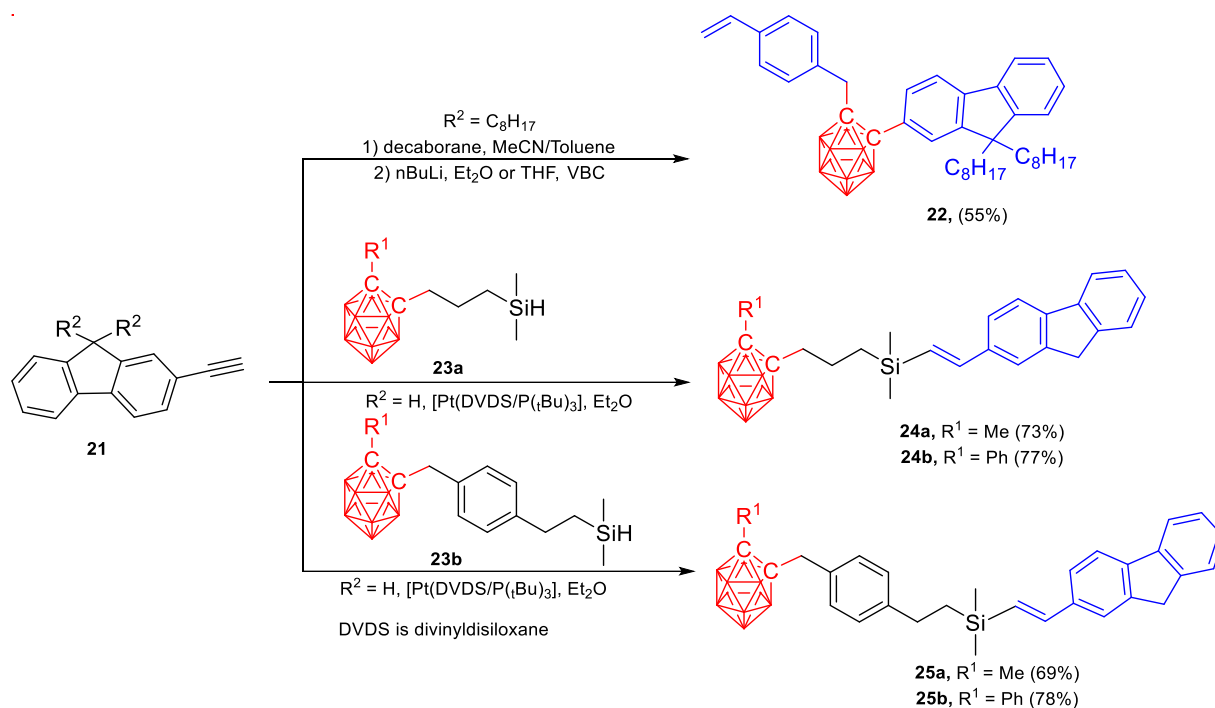
Scheme 8 Synthesis of fluorene-*o*-carboranyl dyads.

H. Yan, Q. Zhao and W. Huang et al. investigated [49] the application in fluorescence microscopy of alkenyl π-conjugated systems with both boron atom and carbon atom modified *ortho-* and *m*-carborane fragments (Scheme 9). The synthetic strategy consisted of two steps, the first of which involved the synthesis of the phenylvinyl derivative **26** from *o*-carborane and 4-iodostyrene in the presence of *n*-BuLi. Subsequent Heck cross-coupling with tri(4-iodophenyl)amine led to the target derivative **27** in 55% yield. It is worth noting that the Heck reaction was used to carry out the B-atom functionalization in the first step. All the obtained compounds showed no significant difference in photophysical properties compared to tri(4-

stilbene)amine: they both absorbed photons in the region of 390–400 nm and emitted in the region of 462-476 nm. Unfortunately, the C-modified *o*-carboranyl substituent exhibited the poorest results of the whole series of compounds. The authors attributed this to the C-C bond of *o*-carborane, which was involved in the excited state and led to the quenching of fluorescence.

However, the B-functionalized *o*-carborane fragment increased the quantum yield from 36 to 55%, and the C-functionalized *m*-carborane enhanced σ to 511 GM. Thus, modification of *o*-carboranyl fragments by B- or C-atom might be used in the directed design of luminescent systems with desired properties.
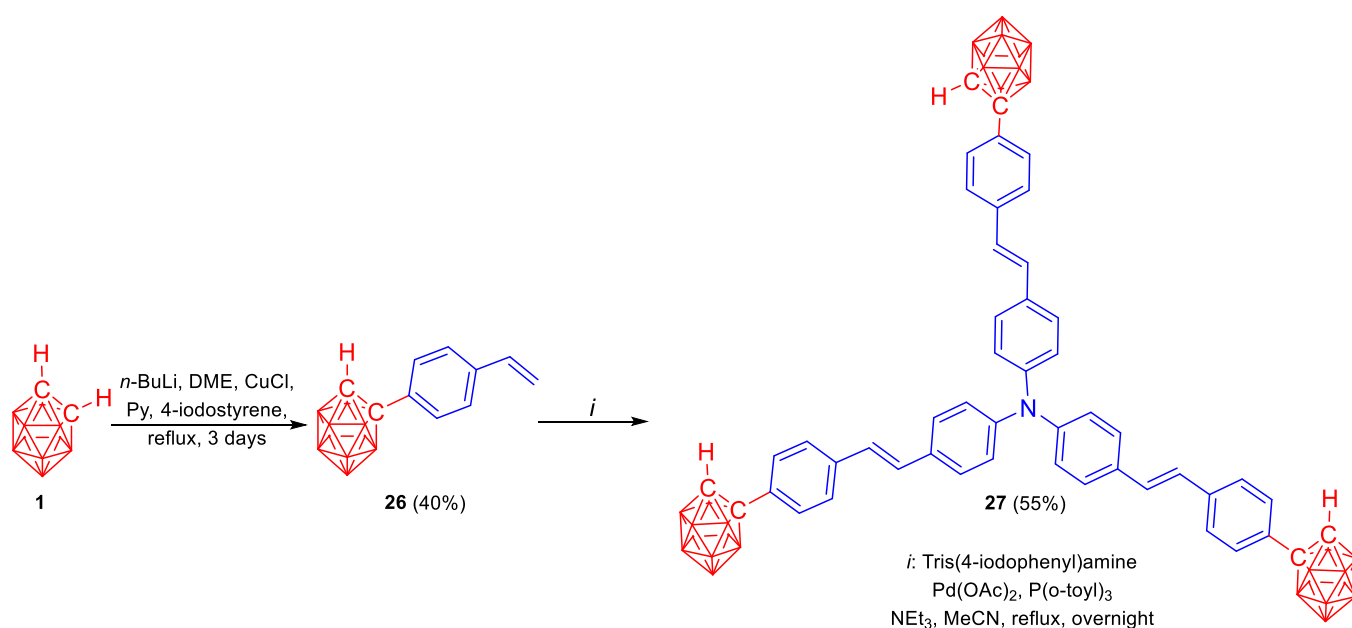
Scheme 9 Synthesis of *o*-carboranyl derivatives of triarylamine.

Our research group [50] developed an approach to the synthesis of triazolyl derivatives of *o*-carborane bonded by an alkenyl spacer. The synthetic strategy included two steps. At the first one vinylacetylene derivative of *o*-carborane was obtained by reaction of *o*-carboranillitium with pyridazine-N-oxide (Scheme 10). The subsequent CuAAC reaction with arylazides led to a series of target compounds **29a–h** in 80–92% yields. The absorption spectra reveal a single band with a maximum at 250 nm; only for compounds **29b** and **29h** a second absorption band at 300 nm was discovered.

The emission spectra showed one narrow band at 316 nm and one broadened band at 380–407 nm. Most likely they could be associated with local excitation (LE) and intramolecular charge transfer (ICT) states (Figure 10). Therefore, due to the developed π-conjugation system, the obtained compounds could be considered as push-pull fluorophores. In addition, the AIEE effect was investigated for compound **29c**. The highest emission intensity is achieved at 90 vol% H_2O, the LE-emission intensity increased 1.8-fold, and the ICT-emission intensity increased 5.3-fold (Figure 11).

Thus, in this section, the methods of preparation and photophysical properties of luminophores based on alkenyl π-conjugated systems have been discussed. The main synthetic technique for their preparation is the Heck reaction of styrene derivative of *o*-carborane. The considered compounds were reported to mainly exhibit blue emission, with the exception of their BODIPY derivatives with emission in the red region. Aggregation properties were observed in almost all cases, but no practical applications in molecular electronics devices have been proposed so far.

3. Luminophores based on alkynyl π-conjugated systems

One of the frequently used *o*-carboranyl moiety in the design of advanced materials with alkynyl π-conjugation system is 1-ethynyl-*o*-carb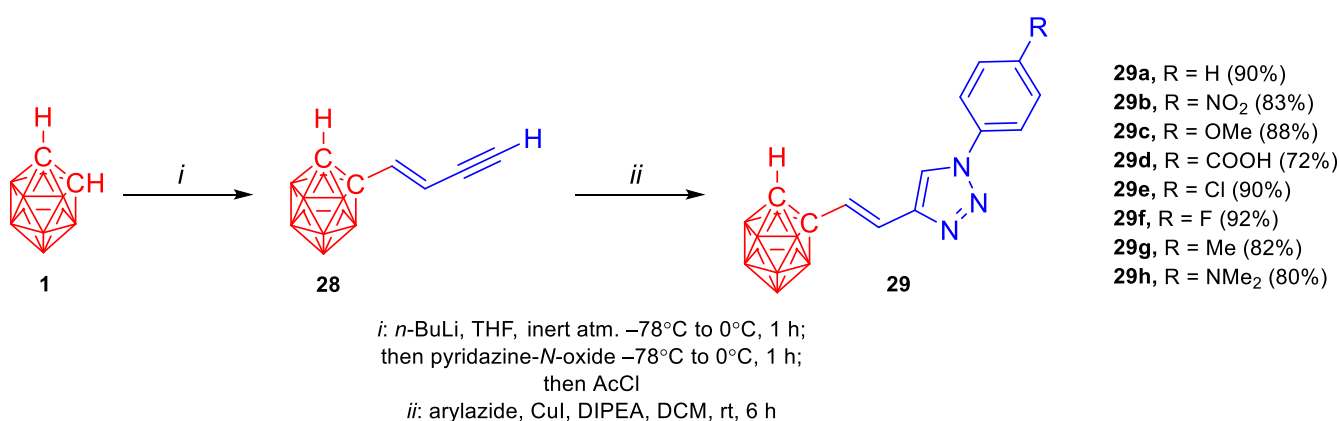orane **31** (Scheme 11–12). It is derived by reaction of *o*-carboranyl copper(I) with (bromoethynyl)triisopropylsilane followed by removal of the silyl moiety. Several research groups were able to obtain mono- and bis(*o*-carboronyl ethynyl)substituted polycyclic (hetero)aromatic derivatives **32–34** in 15–86% yields.
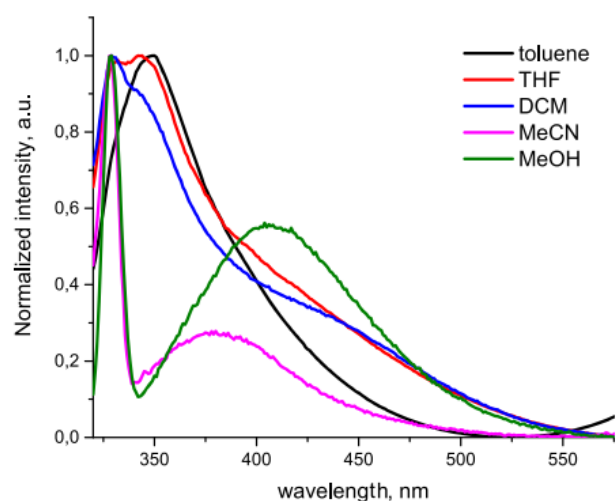
Figure 10 Normalized emission spectra **29h.** Reproduced from L.A. Smyshlyaeva and co-workers [50] with permission from the American Chemical Society.
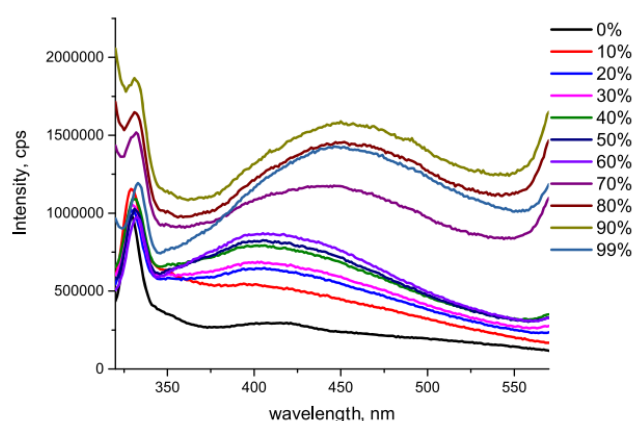
Figure 11 Fluorescence spectra of **29c** in MeOH/water mixtures with different volume fractions of water. Reproduced from L.A. Smyshlyaeva and co-workers [50] with permission from the American Chemical Society.

29a, R = H (90%)
29b, R = NO₂ (83%)
29c, R = OMe (88%)
29d, R = COOH (72%)
29e, R = Cl (90%)
29f, R = F (92%)
29g, R = Me (82%)
29h, R = NMe₂ (80%)

i: *n*-BuLi, THF, inert atm. –78°C to 0°C, 1 h;
then pyridazine-*N*-oxide –78°C to 0°C, 1 h;
then AcCl
ii: arylazide, CuI, DIPEA, DCM, rt, 6 h

Scheme 10 Synthesis of 1,2,3-triazolyl-modified vinylcarborane fluorophores.

i: 1) *n*-BuLi, Et₂O, 0°C than CuCl
    2) (bromoethynyl)triisopropylsilane
ii: KF, TBAB, DCM/H₂O
iii: 1) *n*-BuLi, dry Tol, inert atm., 0°C→rt (12 h);
     then acenequinones, 100°C, 12 h; then H₂O
    2) SnCl₂,Tol, 50°C, 30 min
iv: 1,8-diiodoanthracene, Pd(Ph₃)₄, CuI, THF,
NEt₃, 60°C, 0.5 h, inert atm.
v: polycyclic (het)aryl diiodides, Pd₂(dba)₃, CuI,
TFP, dry THF+Et₃N (1:1), inert atm.

32.1(a–d)
R = H **(a)** (64%^{iii})
R = Me **(b)** (84%^{iii})
R = Et **(c)** (86%^{iii})
R = *n*-Bu **(d)** (85%^{iii})

32.2(a–c)
R = H **(a)** (70%^{iii} / 65%^{v})
R = Me **(b)** (85%^{iii})
R = Et **(c)** (82%^{iii})

32.3, R = H (25%^{iv})

32.4, R = H (37%^{v})

Scheme 11 Synthesis of molecular systems based on derivatives of diacetylenic *o*-carboranes.

i: polycyclic (het)aryl monoiodides,
Pd₂(dba)₃, CuI, TFP,
    dry THF+Et₃N (1:1), inert atm.
ii: 9-bromoacridine, CuI, Pd₂(dba)₃,
P(tBu)₃HBF₄, dry THF⁺Et₃N (1:1), inert
atm.
iii: 9-ethynylacridine, Cu⁰, TMEDA, air,
    CHCl₃+1,4-dioxane (3:1), 50°C, 12 h.

33

34 (15%^{iii})

Examples:

33.1 (61%^{i})

33.2 (36%^{i})

33.3 (13%^{ii})
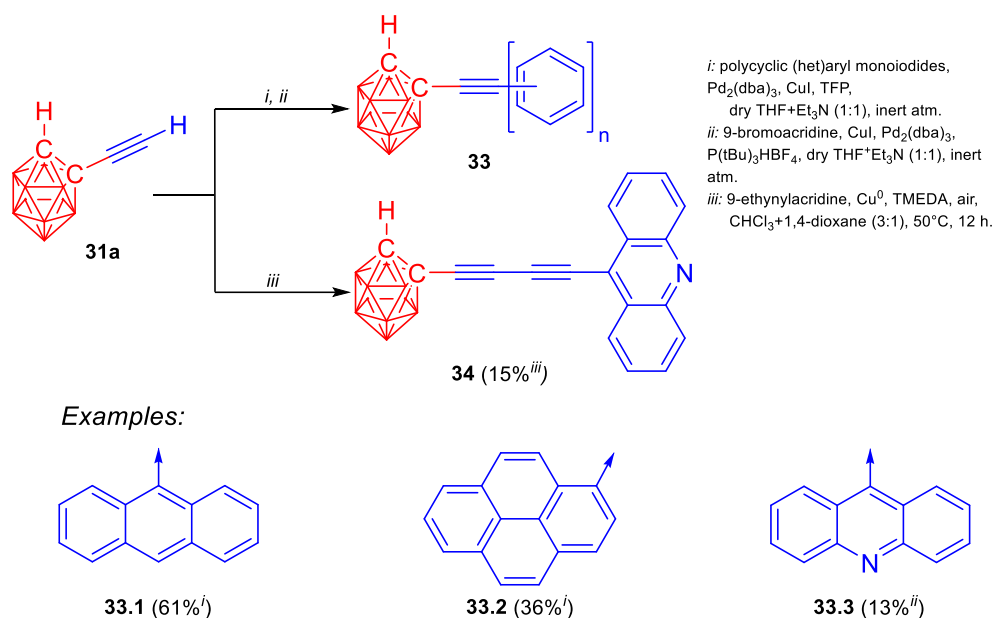
Scheme 12 Synthesis of molecular systems based on derivatives of monoacetylenic *o*-carboranes.

In 2015, Z. Xie et al. proposed [51] disubstituted 6,13-bis(*o*-carboranyl ethynyl)pentacenes **32.1(a–d)** during the molecular design of the ambipolar analog of 6,13-bis(triisopropylsilylethynyl)pentacene (TIPS-pentacene), which is a promising p-type semiconductor. The synthetic strategy was based on the reduction of propargyl alcohols produced in the Favorsky reaction of the anthra- and pentaquinone with *o*-carboranyl acetylenides. The other synthetic strategies were variations of Sonogashira or Glaser-Hay cross-coupling of alkynyl synthons with aryliodides or other alkynes.

Compounds **32.1(a–d)** and **TIPS-pentacene** had two absorption bands in the 250–350 nm and 500–700 nm range; the substitution of TIPS groups to *o*-carboranyl resulted in a bathochromic absorption shift of ~10 nm in the long wavelength region, indicating a higher degree of π-

conjugation of **32.1(a-d)** than TIPS-pentacene. This was most likely due to the involvement of the p-orbital of the C-atom of the *o*-carborane cluster. Thus, replacement of the triisopropylsilyl groups of **TIPS-pentacene** with C-substituted *o*-carboranyl clusters reduced the HOMO/LUMO energy by ~0.3 eV and stabilized them, leading to the enhanced electron mobility and photooxidative stability by 4.6–6.9 times. The authors showed that the choice of alkyl substituent at the second C atom of *o*-carborane affected the molecular packing. In particular, when the butyl substituent was included, it decreased the distance between molecules to the greatest extent.

The thin film transistors based on compounds **32.1(a-b)** displayed insulating properties probably due to weak π-π interactions in the solid state. OTFTs derived from **32.1(c)** exhibited hole semiconductor (p-type) behavior

with field effect mobility ranging from $1.2 \cdot 10^{-4}$ to $1.7 \cdot 10^{-3}$ cm²V⁻¹s⁻¹. Meanwhile, the butyl derivative **32.1(d)** demonstrated the properties of an ambipolar semiconductor with mobility ranging from $2.5 \cdot 10^{-5}$ to $5.5 \cdot 10^{-4}$ cm²V⁻¹s⁻¹ for holes and from $1.2 \cdot 10^{-5}$ to $2.1 \cdot 10^{-4}$ cm²V⁻¹s⁻¹ for electrons. However, the hole mobility results were lower than those of TIPS-pentacene by 4–6 orders, most likely due to the irregularity of the crystal structure of the films (Figure 12).

The subsequent molecular moiety in the design of *o*-carboranyl derivatives of acenes was anthracene **32.2(a–c)** [52]. It was reported that 10-bis(phenylethynyl)anthracene (**BPEA**) is a fluorophore used in organic light-emitting diodes, chemiluminescence sources and optical waveguides. However, its emission in the solid-state is much lower than in solution, most likely due to quenching caused by aggregation-caused quenching (ACQ). Compounds **32.2(a-c)** and **BPEA** have similar patterns of absorption spectra in the 250–320 nm and 350–480 nm regions. The emission spectra of the *o*-carboranyl derivatives displayed a bathochromic shift relative to **BPEA**, namely 462 and 485 vs. 485 and 510 nm, respectively. The authors attributed the bands to the emission of the locally excited (LE) state, which most likely occurs at HOMO→LUMO transitions of the anthracene fragment. It is worth noting that the emission intensity of these compounds decreased significantly in polar solvents (DMF, chloroform, etc.), most probably due to the PET transition from anthracene to the antibonding orbital of the C–C bond of *o*-carborane. The replacement of **BPEA** phenyl groups with C-substituted *o*-carboranyl clusters resulted in a significant decrease in fluorescence quantum yield (from 85.1% to 3.1%). On the other hand, their incorporation caused the occurrence of AIE properties in THF/H₂O mixtures ($f_w \geq 70\%$) with emission maximum at 548–550 nm (Figure 13). In the solid state, **BPEA** and **32.2(a)** emitted at 571 and 572 nm, respectively, while compounds **32.2(b–c)** emitted at 528 and 529 nm, which was ascribed by the authors to different fluorescence mechanisms. For compounds **32.2(b–c)**, the authors suggested a TICT mechanism, while **BPEA** and **32.2(a)** were characterized by the PET transition and ICT state. It is worth mentioning separately that all compounds showed a 10% increase in luminescence lifetime and a ~0.45 eV decrease in HOMO/LUMO gap compared to BPEA.

Therefore, modification of anthracene with *o*-carboranyl clusters allowed one to inhibit π-π-stacking interactions of anthracene fragments and, thus, to reduce ACQ. Meanwhile, the incorporation of an alkyl substituent at the second C atom of *o*-carborane led to a decrease in the C–C bond vibrations of *o*-carborane, in particular the highest $QY_{solid} = 42.9$ % (**32.2(b)**), while $QY_{solid} = 7\%$ for the unsubstituted (**32.2(a)**) (Figure 14).

Another example of disubstituted *o*-carboranyl derivatives of antracene **32.3**, namely 1,8-isomer, was synthesized by K. Tanaka [53]. In addition, the researchers also

obtained a compound without an ethynyl spacer. Both molecules possessed blue emission (~450 nm) in solution and yellow-red (~553-590 nm) in crystal. It is worth noting that the presence of the ethynyl spacer essentially reduced the quantum yield of luminescence in solution and crystal (e.g., 3% for 32.3). The scientists suggested and confirmed by calculations that the emission of **32.3** in the crystal could be assigned as the CT through the ethynylene spacers. On the contrary, the emission in solution of **32.3** was caused only by local excitation, while the molecule without the ethynyl spacer exhibited dual emission attributed to the LE and ICT states. For both compounds, a mechanoluminescence (MCL) phenomenon was detected in case of **32.3** showing hypsochromic MCL effect (up to 495 nm), shifting from CT to excimer emission. In contrast, compound without ethynyl spacer exhibited bathochromic (up to 611 nm) MCL, shifting from dual emission (excimer and CT) to CT emission upon grinding.
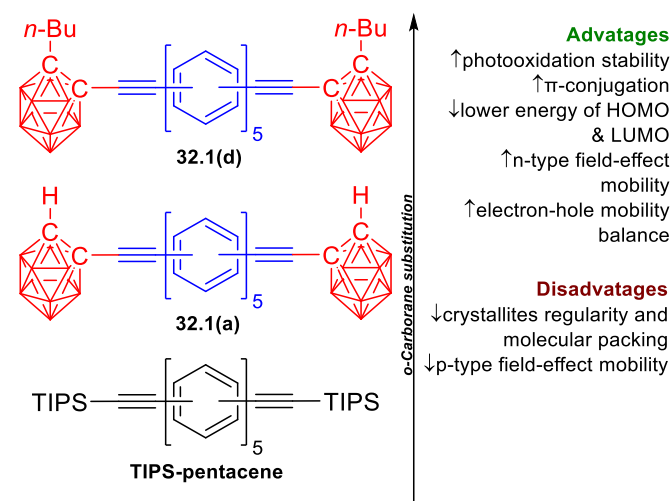
Figure 12 Comparison of the properties of *o*-carboranyl pentacenes with TIPS-pentacene.
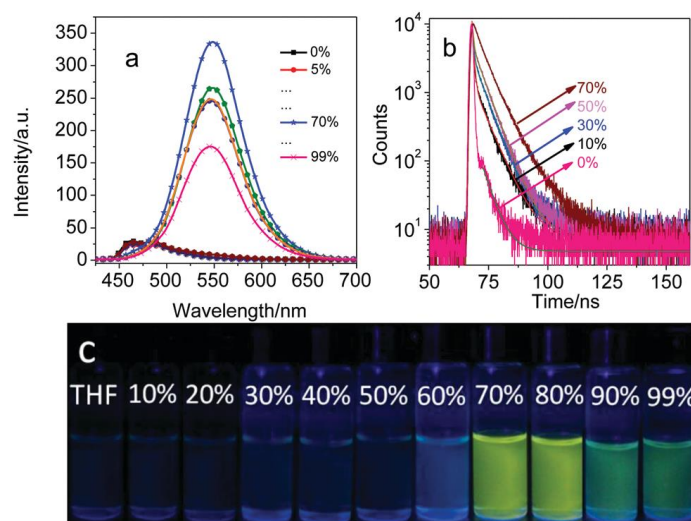
Figure 13 Emission spectra of compound **32.2(b)** with different water fraction (a); lifetime of compound **32.2(b)** in solution with different water fraction (b); photos of compound **32.2(b)** in solution with different water contents. Reproduced from Z. Xie and co-workers [52] with permission from the Royal Society of Chemistry (c).
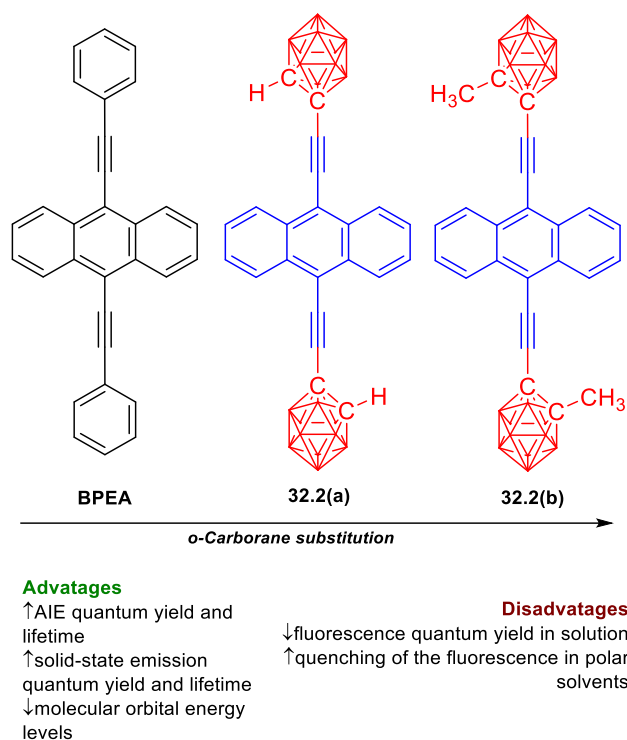
Figure 14 Comparison of the properties of *o*-carboranyl anthracenes with BPEA

Y. Chujo and co-workers [54-56] enlarged the set of polyaromatic *o*-carboranyl compounds by obtaining novel molecules and found unexplored properties of the known mono- and disubstituted pyrenyl and anthracene derivatives **32.4, 33.1, 33.2**. It was discovered that the disubstituted anthracene derivative could form two kinds of crystals (G- and Y-forms) with green and yellow emission, respectively. The authors found that the G-form crystals are dominated by the LE state, while the Y-form crystals possess the ICT state with longer lifetime. In addition, G crystals were larger (5–20 μm) in size than Y crystals (1–5 μm) (Figure 15).

Meanwhile, the monosubstituted (Scheme 12) anthracene derivative **33.1** exhibited a hypsochromic shift of 20 nm in the absorption and emission spectra with an approximately equal band pattern as **32.2**. The emission spectra in solutions showed only the LE state, while emission in the solid state was accompanied by the ICT state. The quantum yields did not exceed 1%, whereas they reached 12% for the disubstituted derivative. The authors observed mechanoluminescence (MCL), in which mechanical action had led to a color change of emission from orange to green, while heating or effect of chloroform vapor led to yellow emission in the solid state (Figure 16).

The monosubstituted pyrene derivative **33.2** possessed absorption in the 350–386 nm range and emission in the blue region up to 450 nm. The emission most probably belonged to the LE state, while the ICT state was found when the emission spectra were investigated under delayed rotation conditions (at 77 K). It is worth mentioning

that in the absence of the alkynyl spacer the emission was accompanied by the ICT state even at room temperature. In addition, the authors investigated the time-dependent increase in emission intensity (TDEE). The freshly prepared fluorophore solution in THF showed about zero quantum yield; after 120 h, the QY increased more than 15 times. This was most likely due to the formation of photoactive pyrene excimer, which may depend on the amount of water in the solvent. The authors proposed a possibility of using this property for chemosensor determination of water content in the organic solvent. Depending on the amount of water, the color and intensity of the emission change, namely up to 5% H_2O a blue emission was observed, from 5 to 20% the emission changes to white light; however, more than 20% water content could not be found (Figure 17).

Meanwhile, the disubstituted pyrene derivative **32.4** demonstrated a spectral pattern similar to that of **33.2**.
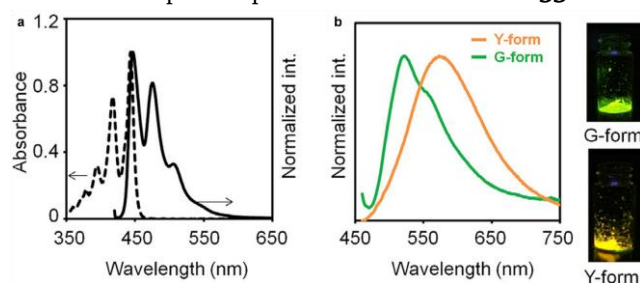
Figure 15 Optical properties of **32.2(a)** (dCBEA) (a) Absorption and emission spectra in THF ($1.0 \cdot 10^{-5}$ M) (b) Emission spectra of crystals in G and Y forms. Reproduced from Y. Chujo and co-workers [56] with permission from the Elseiver.
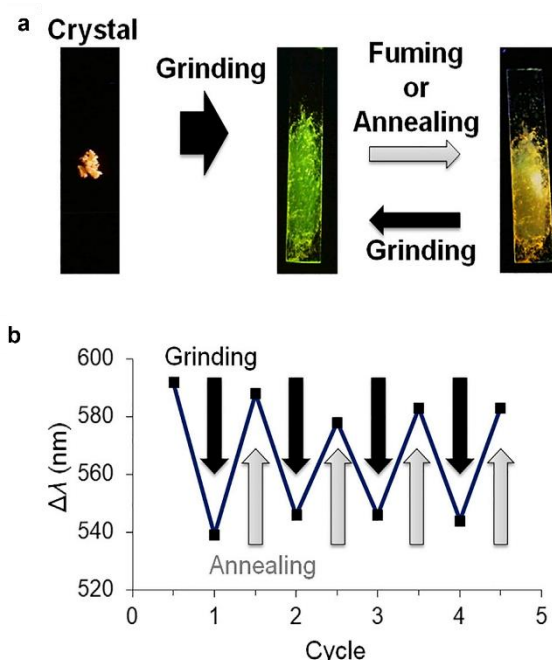
Figure 16 Luminochromic behavior of **33.1** (CBEA) (a) solid-state luminescent chromism toward various stimuli. Photos were taken under UV irradiation (λ_{ex} = 365 nm); (b) reversibility in the grinding and annealing cycles. Reproduced from Y. Chujo and co-workers [56] with permission from the Elseiver.
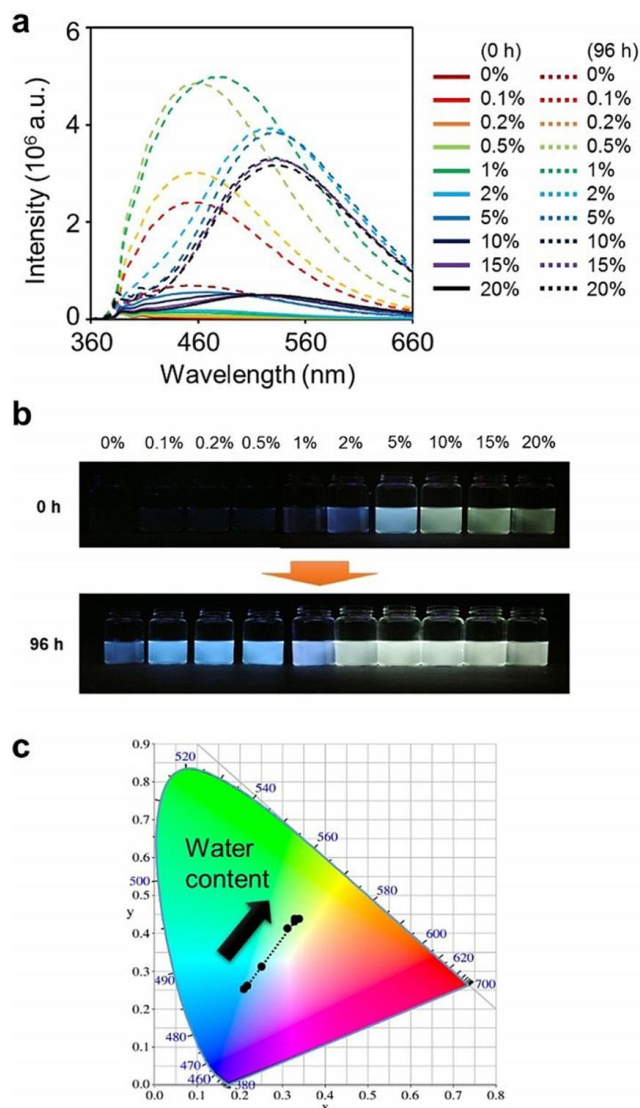
Figure 17 (a) Emission spectra of **33.2**; (b) photos were taken under UV irradiation (λ_{ex} = 365 nm). of acetone solutions with different water fraction after 96 h at 25 °C (c) luminescent colors of the solutions on the CIE diagram. Reproduced from Y. Chujo and co-workers [55] with permission from the Wiley.

A significant change was found, as **32.4** could form two kinds of crystals (Y- and O-type). Their luminescence was almost identical, but the O-type was more thermodynamically stable. The authors reported that these crystals showed mechanoluminescence, and the emission depended on the type of mechanical action. For example, when lightly tapping the color changed from orange to yellow, and when rubbing the emission became green, which was most likely due to excimer emission. In order to recover crystals with yellow emission, the compound had to be heated to 120 °C or exposed to toluene vapor (Figure 18).

The last example of acene derivatives of *o*-carborane is acridine. Y. Chujo et al synthesized several acridine [57–58] derivatives containing one **33.3** or two alkynyl spacers **34**. The spectral characteristics of these homologues were nearly similar, possessing absorption in the 370-420 nm region, blue emission in solution (420–450 nm) and yellow-red emission in the solid state (574–610 nm). The emission behavior in solution most likely referred to the

LE state, whereas the ICT state was found at 77 K in 2-MeTHF when the molecular rotation was sufficiently slowed down. Meanwhile, the emission in the solid state was attributed to the forming of intermolecular excimers by the spatial interaction of C_{cage}-H with the nitrogen of the acridine ring. With increasing conjugation system, the HOMO/LUMO energy difference decreased and thus the QY in solution **34** increased threefold to 21%. In contrast, in the solid state, the QY was larger at **33.3** (23%) owing to the shorter distance between the carborane and acridine moiety in the excimers.

The authors also found that a hypochromic shift of emission occurs with increasing temperature and the intensity decreases significantly. Most likely, such thermochromic luminescence was caused by the gradual dilation of the crystal lattice and an increase in non-radiative transitions. The researchers also suggested using this feature as a temperature chemosensor (Figure 19).
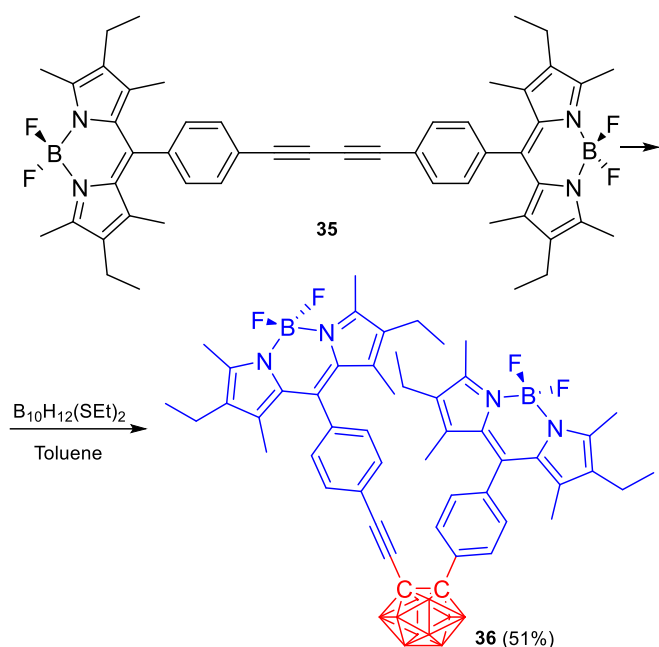
From the ethynyl derivative of *o*-carborane, S.O. Kang et al. [59] developed BODIPY fluorophores. Decaborane (**14**) strategy with diethynyl derivative was used for their synthesis. The yield of the target molecule was 51% (Scheme 13). The authors also obtained analogs without ethynyl spacer and without carboranyl spacer. All compounds had almost exactly the same spectral characteristics, absorbing photons in the 320–520 nm range, and emission was recorded in the 544 nm region.
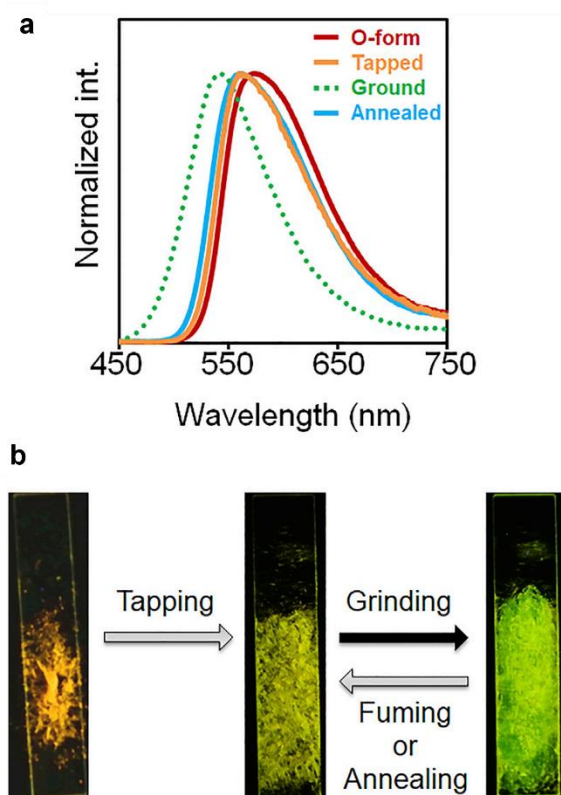
Figure 18 Luminochromic behavior of **32.4** (dCBEP) (a) solid-state luminescent chromism toward various stimuli; (b) Photos were taken under UV irradiation (365 nm). Photos were taken under UV irradiation (λ_{ex} = 365 nm). Reproduced from Y. Chujo and co-workers [56] with permission from the Elseiver.
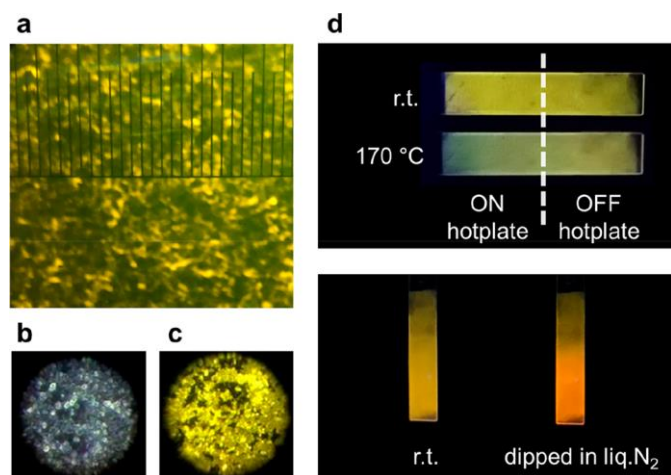
Figure 19 Fluorescence microscope image (100×) of an **33.3** dispersed quartz substrate (a). Minimum scale value: 0.05 mm. Dark field (b) and fluorescence microscope images (1000×) (c). Thermoresponsivity of **33.3**-dispersed quartz substrate (d). Reproduced from Y. Chujo and co-workers [57] with permission from the Americal Chemical Society.


**Scheme 13** Synthesis of o-carboranyl derivative of di-BODIPY.

The incorporation of o-carborane cluster led to a significant decrease in QY from 62% to 23% while the presence of ethynyl spacer in o-carboranyl derivatives reduced QY by only 8%. In addition, the same tendency was observed when measuring the fluorescence lifetime: **36** had τ = 1.4–1.8 ns, while the carboranyl-free ones reached 4 ns. This was attributed to PET processes from the BODIPY fragment to o-carborane. The authors also found that such structures can produce radical particles, which may be useful in photodynamic therapy of tumors.

The next structure, from which various functional materials containing a triple bond could be obtained, was an alkynyl derivative of o-carborane with a phenylene spacer. For the first time its use was suggested by Y. Chujo [60–61] and coworkers as a structural unit in AIE photoactive polymers. The synthesis strategy involved the Sonogashira

reaction between the diiodo derivative of o-carborane **37I** and dialkynylaryls **38a–e**. Five optically active polymers **39a–e** were obtained in 80–94% yields (Scheme 14). The number-average molecular weights of the polymers were in the range of 2800–3800 Da. The prepared polymers exhibited absorption in THF solutions from 338 to 380 nm, and emission in the blue region with almost zero quantum yield. However, when aggregates were formed in THF/H$_2$O mixtures, a bathochromic shift of emission to the yellow region up to 583 nm and an increase in QY from 2 to 12% were observed (Figure 20). The exception was the polymer with EWG substituent **39d**, the emission of which was in the blue region ~485 nm. Besides, it would be interesting to note the authors' findings on the synthesis of optically active polymers **39e**: it was found that the presence of o-carborane provides them with AIE-properties and emission in thin films, while their m-carboranyl analog led to photoactive compounds in solutions.
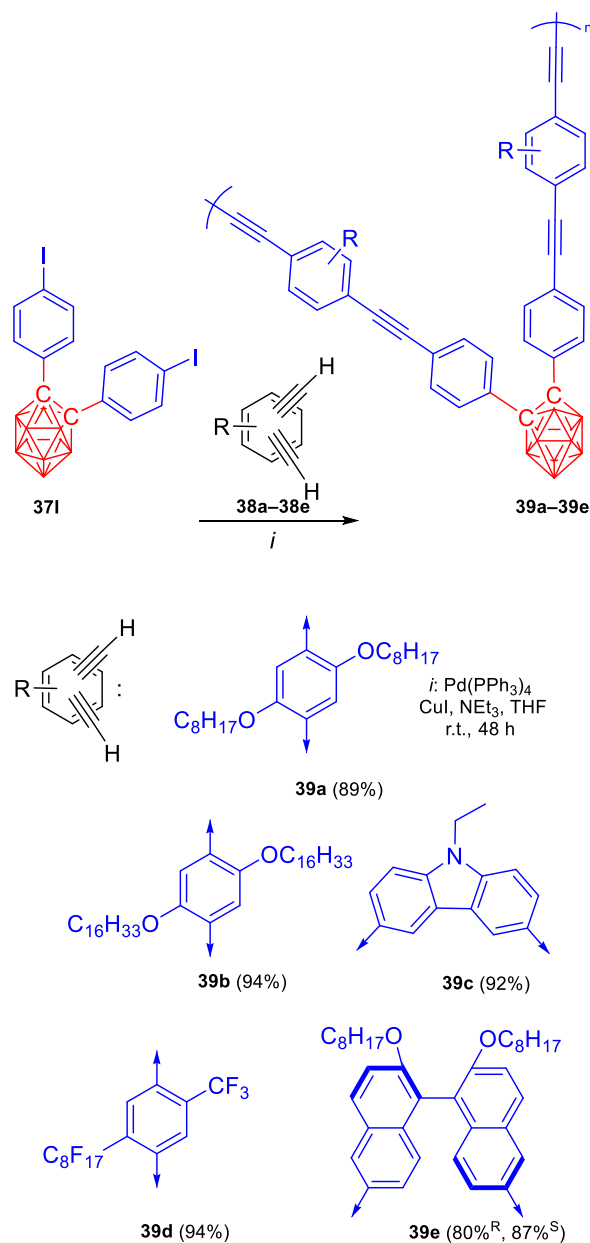
Scheme 14 Synthesis of polymers based on 4-ethynylphenyl-o-carborane.
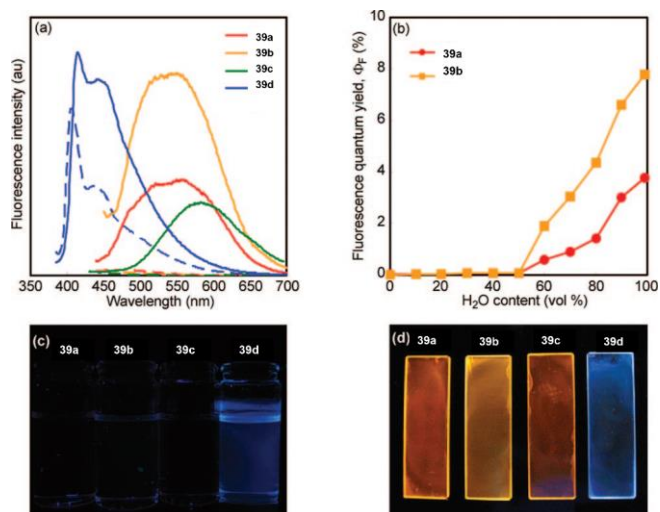
Figure 20 Fluorescence spectra of **39a–39d** in THF ($1·10^{-5}$ mol/L, dashed line) and mixed solvent of THF/H_2O = 1/99 (v/v) ($1·10^{-5}$ mol/L, solid line) (a). Dependence of quantum yields of **39a** and **39b** on solvent compositions of the THF/H_2O mixture and photographs of **39a–d** (b) in solution state (c) and in film state (d). Reproduced from Y. Chujo and co-workers [61] with permission from the American Chemical Society.

The authors suggested that the *o*-carboranyl moiety contributes to the restriction of vibrational rotations in polymers. Thus, this *o*-carboranyl fragments can be exploited for fine-tuning of ordered polymer structures.

Y. Chujo et al. [62] also proposed a technique to modify (*p*-phenylene-ethylenyl) (PPE) based polymers **40** with *o*-carboranyl cluster via decaborane (**14**) synthesis strategy. The obtained polymers **41a–c** had number-average molecular weights up to 4900 Da, absorbance at 419–431 nm and blue emission in the region from 470–497 nm. The modification of PPE with an *o*-carborane cluster led to the ICT state and AIE properties and improved the thermal properties of the polymers (Scheme 15).

Following the research on carboranyl-containing polymers, Y. Chujo et al. [63] suggested a method for the synthesis of uncommon derivatives based on benzocarborane **42**. The obtained polymers **44** had a molecular mass up to 22700 Da, while monomers **43a** with EDG polymerized more readily than with EWG **43b** (DP 23.9 and 8.1, respec-
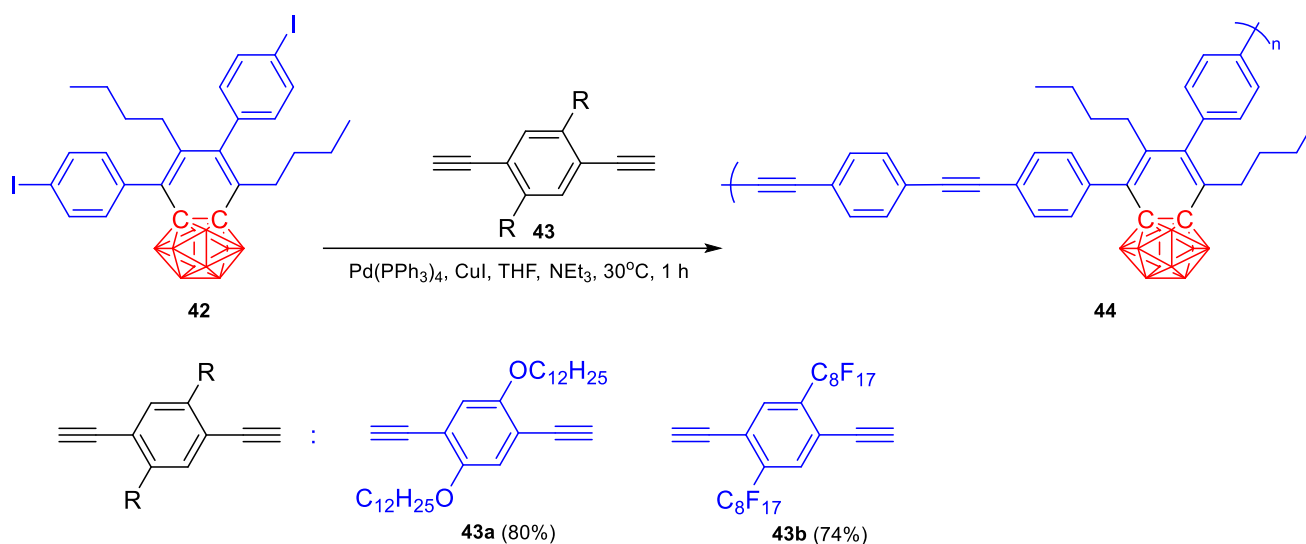
tively). Absorption of these macromolecules was observed in the 330–410 nm region, and emission was recorded in the blue region of 420–460 nm with a QY of 40–51%. The authors show that these fluorophores represent a D-π-A system in which the benzocarborane moiety served as an acceptor. In addition, it was found that the incorporation of the carboranyl fragment decreased the energy of molecular orbitals and did not affect the fluorescence efficiency, most likely due to the lack of free rotation of the boron cluster (Scheme 16).

Y. Chujo et al. in 2009 [64] proposed a method for obtaining this structural block with a phenyl substituent **46a**, and then in 2011 [65] expanded the applicability of the approach, obtaining six additional new derivatives **46f–k**. A significant expansion of the series was achieved by using in the Sonogashira reaction of the corresponding aryl bromide instead of aryliodide. The authors disclosed that the compounds absorbed light in the region of 300–350 nm. The longest absorption wavelength was detected for compound **46j** containing the electrondonating group of dimethylamine. The emission of the compounds was discovered from 400 to 750 nm, which was directly dependent on the strength of the EDG on the other side of the push-pull system. The quantum yields were in the range of 1–31%. It is worth noting that compound **46a** had almost no quantum yield, but its QY increases to 27% when forming H-aggregates with a size of 107.8±23.0 nm. In addition, the emission of the obtained aggregates was selectively quenched by nitrobenzene, which makes them promising for application as chemosensors for the determination of nitroaromatics.
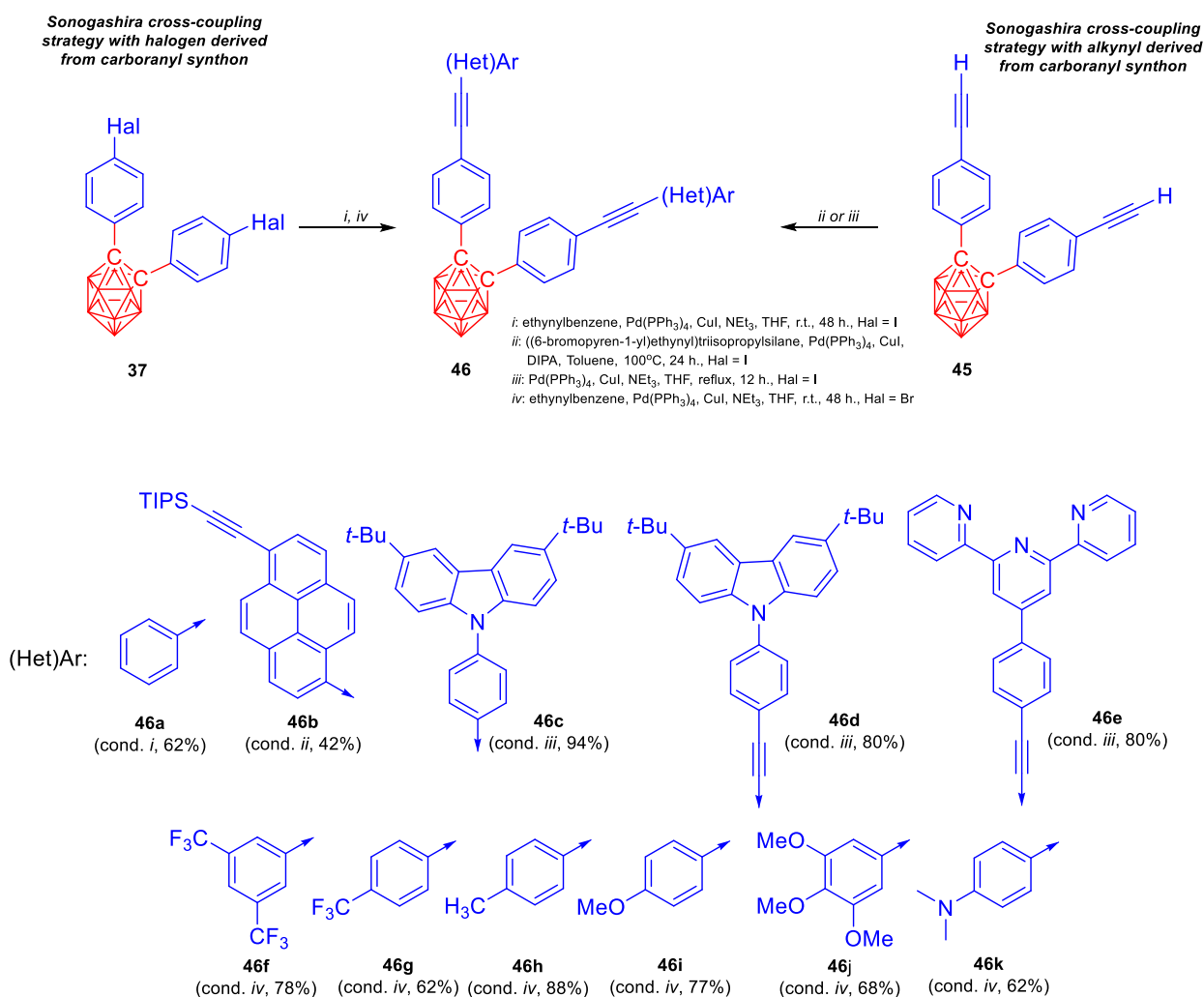
Several scientific groups further investigated photoactive materials based on 1,2-bis(4-ethynylphenyl)-*o*-carborane. As the primary synthetic approach, the Sonogashira reaction was employed in two variations: one with the alkynyl moiety as part of the *o*-carboranyl synthon **45** and the other without (Scheme 17). There were eleven compounds **46a-k** with similar yields obtained.
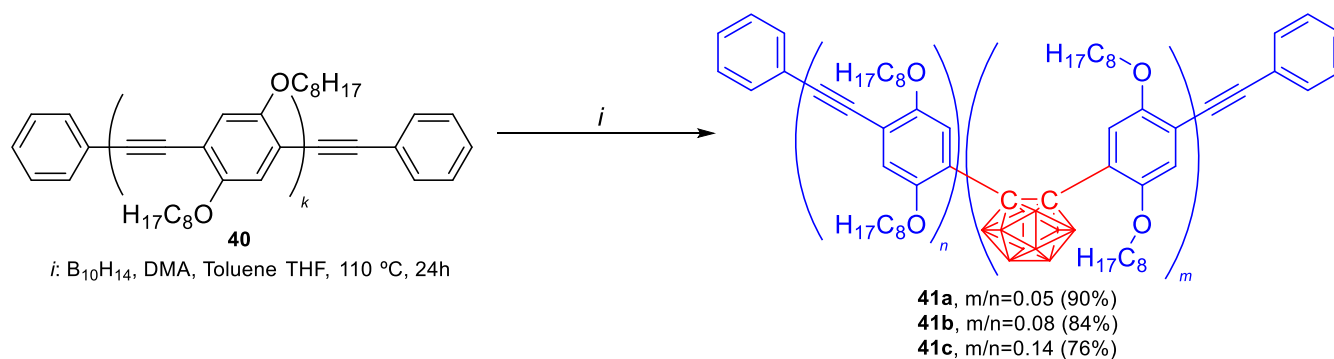
Scheme 15 Synthesis of PPE polymers modified with *o*-carborane.

Scheme 16 Synthesis of polymers based on benzocarborane.

i: ethynylbenzene, Pd(PPh₃)₄, CuI, NEt₃, THF, r.t., 48 h., Hal = I
ii: ((6-bromopyren-1-yl)ethynyl)triisopropylsilane, Pd(PPh₃)₄, CuI, DIPA, Toluene, 100°C, 24 h., Hal = I
iii: Pd(PPh₃)₄, CuI, NEt₃, THF, reflux, 12 h., Hal = I
*iv*: ethynylbenzene, Pd(PPh₃)₄, CuI, NEt₃, THF, r.t., 48 h., Hal = Br

Scheme 17 Synthesis of luminophores based on 1,2-bis(4-ethynylphenyl)-*o*-carborane.

H. Peng and Y. Fang et al. [66] developed a procedure for the preparation of (bis)pyrenyl derivative of *o*-carborane **46b** to use as a chemosensor for the detection of volatile organic compounds (VOCs). The compound exhibited absorbance in the 388–415 nm range, emission of up to 645 nm and a QY of 18–74% depending on the polarity of the solvent. The authors suggested that the emission of fluorophores was associated with an intramolecular charge transfer (ICT) state, which was stabilized by the polar solvent and thereby decreased the QY. It is worth mentioning that in low-polar solvents (hexane, CCl₄) a local excitation (LE) state was also observed, which was a distinctive feature of push-pull fluorophore systems [67]. When aggregates were formed in THF/H₂O solution, an

increase in quantum yield of up to 26% was found, while in thin films the quantum yield was 36% with a lifetime of up to 7.5 ns. The authors proposed the possibility of using different emission wavelengths to detect hexane, CCl₄, toluene, dioxane vapors, and also to determine the octane number of gasoline (Figure 21). The emission of compound **46b** in the tested gasoline samples ranged from light pink to bright yellow for 92 and 98 gasoline, respectively (Figure 22).

C. Zhang and M.G. Humphrey et al. [69] proposed similar heterosubstituted fluorophores **46c** as well as molecules with an enhanced conjugation system **46d**. The compounds were found to have multiple absorption bands from 295 to 368 nm and to emit in the area of up to 632 nm. It is worth noting that a bathochromic shift (~ 20 nm) was observed depending on solvent polarity, and a state of dual emission was observed in toluene. The authors attributed these properties to the fact that the molecules could be in the LE and ICT states.
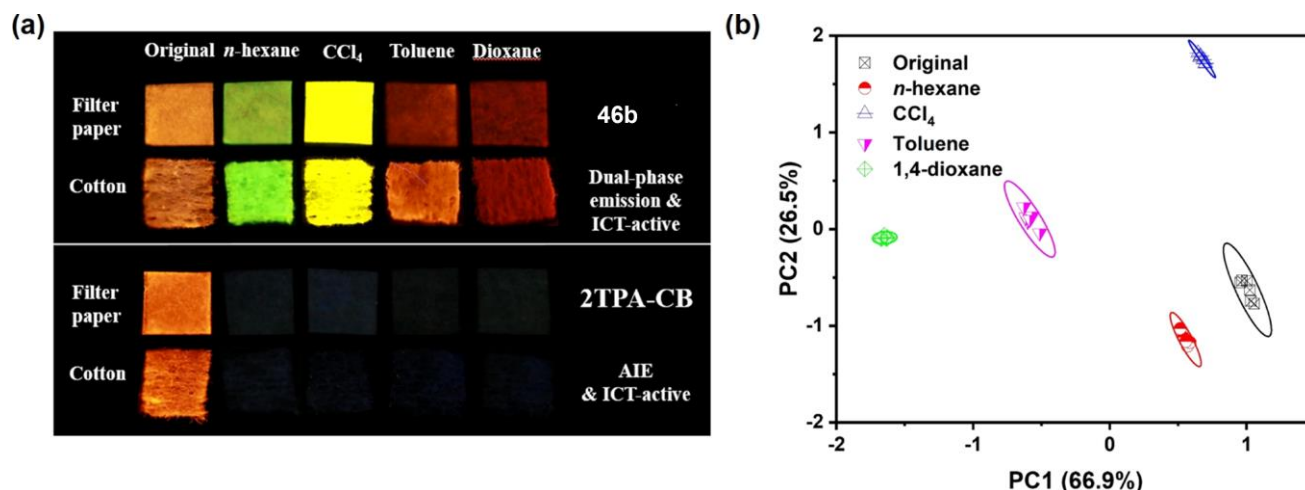
Figure 21 Fluorescence images of **46b** (up) and the reference compound 2TPA-CB (1,2-*bis*(4-(diphenylamino)phenyl)-*o*-carborane) [68] (down) based on test strips with filter paper and cotton cloth as substrates (~0.5 cm·0.5 cm) before and after dipping in different VOCs. The photos were taken under UV light (λ$_{ex}$ = 365 nm) (a). Two-dimensional PCA score plot for discriminating four solvents by using the RGB values of the **46b**-based test strips with filter paper as a substrate during visualization (b). Reproduced from Y. Fang and co-workers [66] with permission from the American Chemical Society.
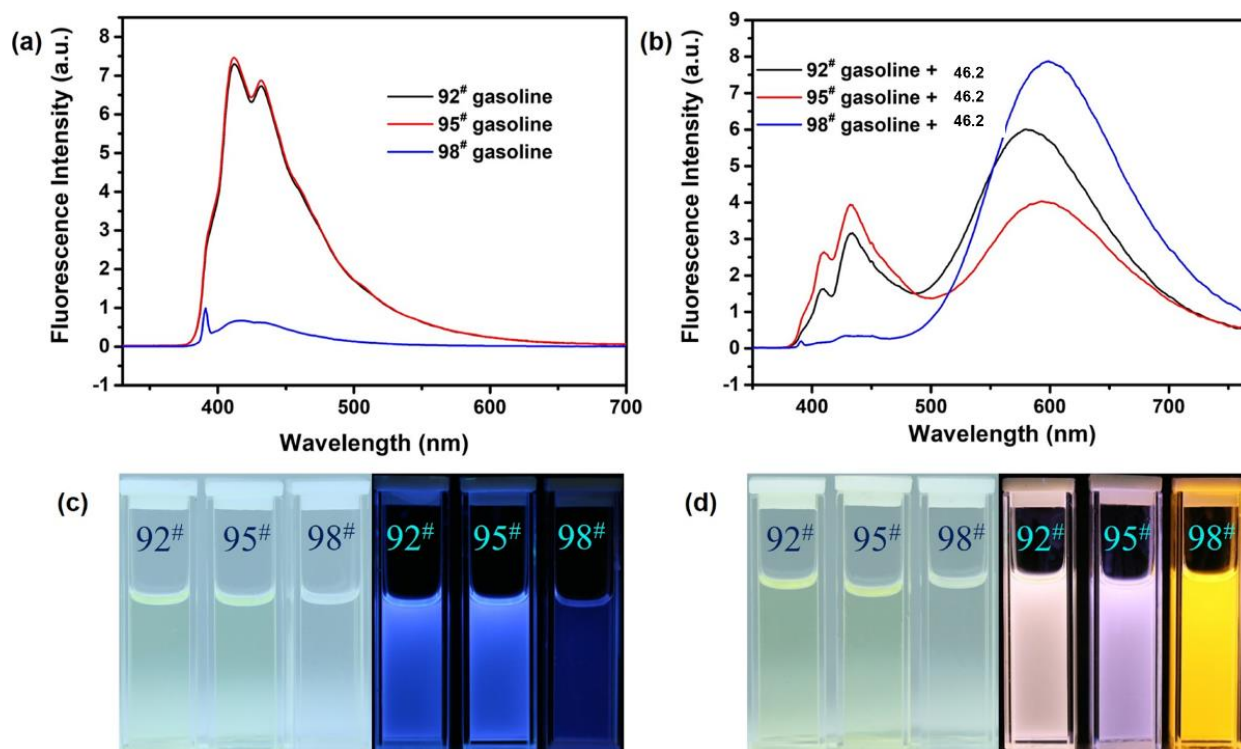

Figure 22 Fluorescence emission spectra of the pure gasolines (92#, 95#, 98#) (a) and 3 mL of gasolines (92#, 95#, 98#) with 30 µL of the dichloromethane solution of **46b** (1·10⁻⁴ mol/L) with 390 nm as the excitation wavelength (b). Images of (c) 92#, 95#, and 98# gasolines under visible light and UV irradiation (λ$_{ex}$ = 365 nm) and (d) 92#, 95#, and 98# gasolines with CB-PY under visible light and UV light (λ$_{ex}$ = 365 nm). Reproduced from Y. Fang and co-workers [66] with permission from the American Chemical Society.

Modification of this system with a terpyridine fragment [70] led to the creation of ligand systems that could be used for fluorescence detection of zinc cations. Compound **46e** had absorption in the region of 300–350 nm and yellow emission; in the presence of the analyte a bathochromic shift of emission to the blue region (turn-on fluorescence) was observed (Figure 23). The authors suggested that the obtained fluorophore is a push-pull system in which the *o*-carboranyl moiety acts as an acceptor and the emission was driven by the ICT state. An intraligand charge transfer state from the *o*-carboranyl cluster to the zinc ions is detected when the metal complex was formed in a 1:1 ratio. In addition, they determined the properties of AIE that allow analyzing the metal in aqueous solutions.
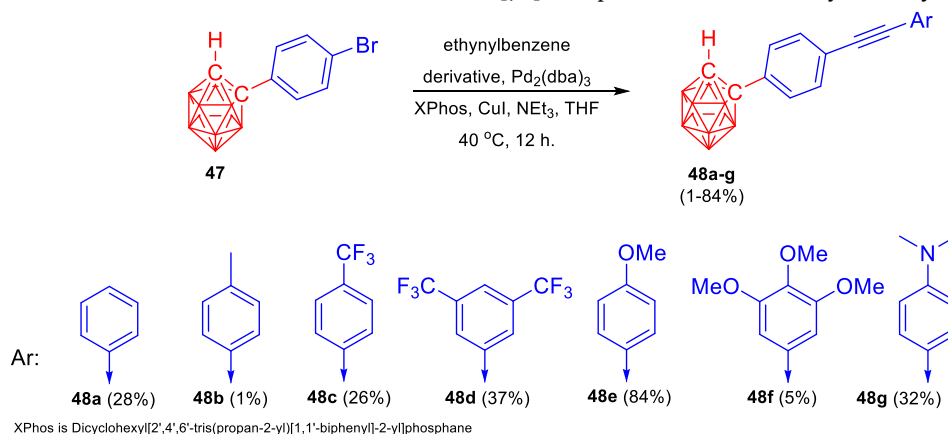
Y. Chujo et al. carried out [71] further research on *o*-carboranyl fluorophores and suggested a procedure for the preparation of monosubstituted tolan derivatives **48a–g**. The researchers obtained a series of derivatives with substituents of different nature with yields from 1% to 84% (Scheme 18). These fluorophores appeared to be a push-pull system in which the C-substituted *o*-carboranyl fragments acted as an EWG. A dual emission phenomenon was observed in the emission spectra from 325 to 600 nm, which is attributed to the emission of CT and ICT states. In addition, the authors also found thermochromic properties of the molecules, in contrast to the results of Y. Fang. In this case, a decrease in the emission intensity with increasing temperature was detected.

In two studies by K. Tanaka and Y. Chujo [72–73] developed a series of bis-*o*-carborane-substituted 1,4-bis(thienylethynyl)benzene **50a-b** and 1,4-bis(phenylethynyl)benzene **50c-d** using decaborane synthesis strategy, while the yields were slight and did not exceed 20% (Scheme 19). Both series of compounds exhibited double emission consisting of LE and TICT in the blue and yellow-red region, and were capable of the aggregate formation. It is worth noting that **50c-d** molecules possessed significantly higher QY (up to 78%) compared to **50a-b** (up to 18%). Solvatochromic and thermochromic properties were discovered for all molecules, which are characterized by an increase in the intensity of emission
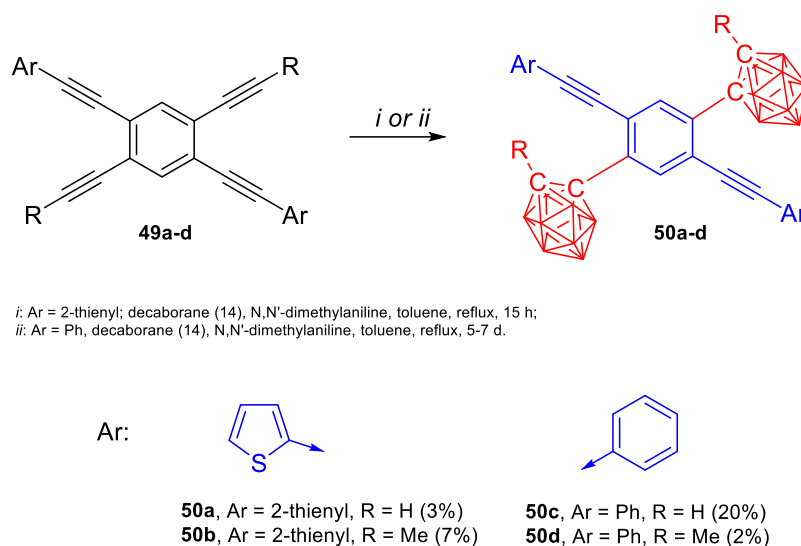
with increasing temperature. For compounds with a thienyl substituent, mechanochromic properties with a bathochromic shift of emission were found. Based on **50a–b**, thin films were prepared that could be utilized as luminescent thermometers. Meanwhile, for the phenyl derivatives **50c–d**, the TICT effect was disclosed even in the solid state, and a crystallization-induced emission enhancement (CIEE) effect was detected, which was mentioned for the first time in this review. The authors suggested that these effects can be attributed to the suppression of aggregation-caused quenching (ACQ) by the bulky cage structure and the spherical shape of o-carborane. It should be noted that mechanoluminescence properties from the series of **50c–d** were found only for compound **50d**, containing a methyl moiety in the *o*-carborane fragment (Figure 24). The observed phenomenon could be due to the presences of the alkyl substituent organizing the crystal packing.
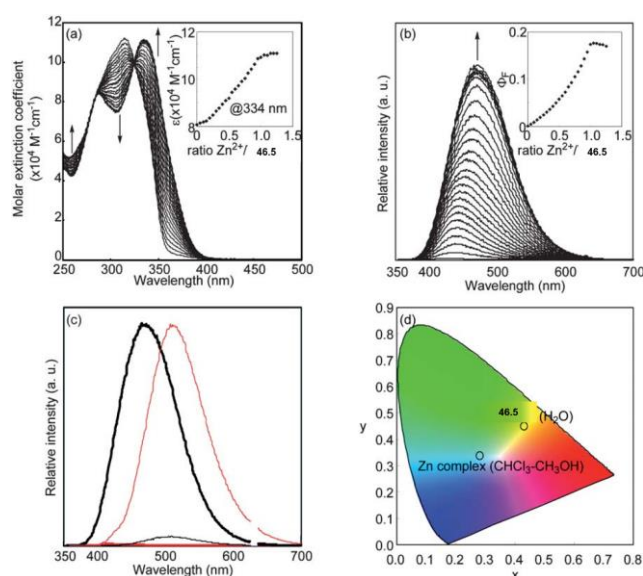

Figure 23 (a) UV-vis and (b) fluorescence spectra obtained by the titration of **46e** in CHCl$_3$–CH$_3$OH (60:40; 1.0·10^{-5} M) with Zn(OAc)$_2$·2H$_2$O. The inset shows (a) the molar extinction coefficient at 334 nm and (b) fluorescence quantum yield as a function of Zn(II)/**46e** ratio. (c) Fluorescence spectra of **46e** (red) and the Zn complex (black) in CHCl$_3$–CH$_3$OH (60:40; 1.0·10^{-5} M, bold line) and mixed solvent of THF–H$_2$O (1:99, 1·10^{-5} M, thin line); (d) CIE 1931 (x,y) chromaticity diagram of **46e** and the Zn complex from the fluorescence spectra. Reproduced from Y. Chujo and co-workers [70] with permission from the Royal Society of Chemistry.

XPhos is Dicyclohexyl[2',4',6'-tris(propan-2-yl)[1,1'-biphenyl]-2-yl]phosphane

Scheme 18 Synthesis of *o*-carboranyl tolanic derivatives.

i: Ar = 2-thienyl; decaborane (14), N,N'-dimethylaniline, toluene, reflux, 15 h;
ii: Ar = Ph, decaborane (14), N,N'-dimethylaniline, toluene, reflux, 5-7 d.

Ar:

50a, Ar = 2-thienyl, R = H (3%)   **50c**, Ar = Ph, R = H (20%)
50b, Ar = 2-thienyl, R = Me (7%)   **50d**, Ar = Ph, R = Me (2%)

Scheme 19 Synthesis of bis-*o*-carborane-substituted 1,4-bis(thienylethynyl)benzene and 1,4-bis(phenylethynyl)benzene.
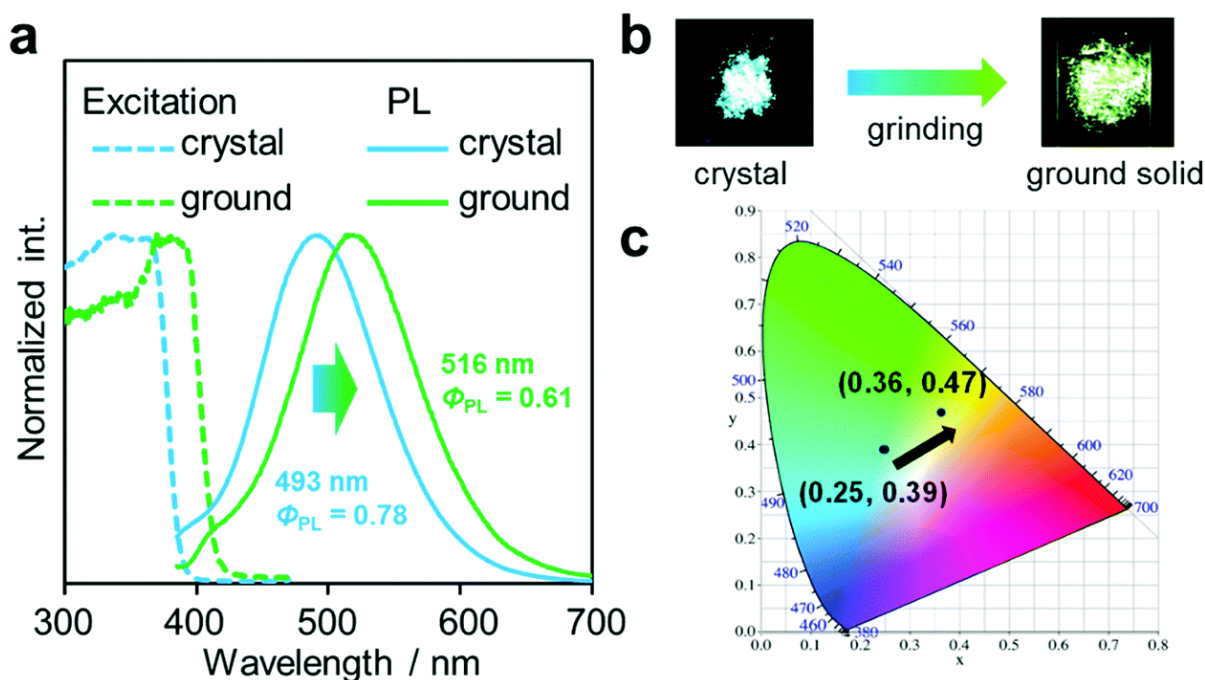
Figure 24 (a) PL and excitation spectra of the solid samples of **50d**; (b) Pictures of the solid samples under UV irradiation before and after grinding; (c) Luminescent colors of the samples on the CIE diagram. Reproduced from Y. Chujo and co-workers [73] with permission from the Royal Society of Chemistry.

Rylene diimides are a class of organic molecules characterized by electron withdrawing and conductive properties, which have been utilized to synthesize many dyes, fluorophores, chemosensors, and other useful molecular electronics materials. These diimides include pyromellitic diimide, naphthalenediimide, pyrene diimide, and perylenediimide [74–75] (Figure 25).

Y. Fang et al. prepared several luminescent compounds with functional properties on the basis of mono- and disubstituted *o*-carboranyl moiety **51.1-3** and perylene dimiimide (Scheme 20). In all cases, the Sonogashira cross-coupling with haloarenes under typical conditions was utilized with yields of 42–90%. The researchers [76] first obtained compound **52** as well as its analog without the alkynyl spacer. The molecules possessed absorption in the region of 500-560 nm, double

emission from 550 to 700 nm, and QY of up to 57%. The authors proved that the first emission band belongs to the emission of a single molecule, while the second band is the emission of excimers. It is worth noting that an uncommon result for similar compounds was the temperature-dependent increase in emission intensity. This temperature sensitivity of fluorophores could be used in the design of chemosensors for living organisms.

Further work [77] of the researchers focused on unfunctionalized structures **53** as well as their monosubstituted ones **54** and dimers **55–56**. The compounds modified by the diimide substituent possessed two sets of absorption bands in the region of 350 and 500–550 nm, while the second set of bands was absent for the unmodified one.
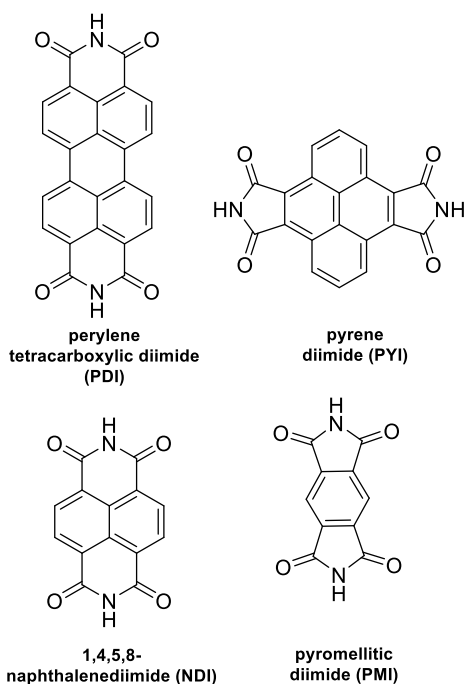
Figure 25 Diversity of rylene diimides

The emission wavelength depended on the polarity of the solvent and was from yellow to red range; the quantum yields were high and reached 91%. In addition, emission was also detected upon excitation with different wavelengths, which was most likely due to the steric alterations that the molecule undergoes in the excited state (Figure 26). The authors developed a sensor device based on thin films of fluorophores capable of detecting volatile organic compounds; the optimal response was detected in the presence of amines (methylamine, dimethylamine, trimethylamine, ethylamine), which could generally be used to assess the freshness of products, in particular fish (Figure 27). The device was composed of a solenoid valve, optical and gas chambers, a tube system and an electronic system for analyzing the results. In the presence of the analytes, the fluorescence intensity decreased almost until the emission disappeared. The mechanism of quenching was similar to the one described in the authors' previous study and refers to photoinduced electron transfer from electron-donating amino derivatives to electron-accepting *o*-carboranyl fragments in the excited state.
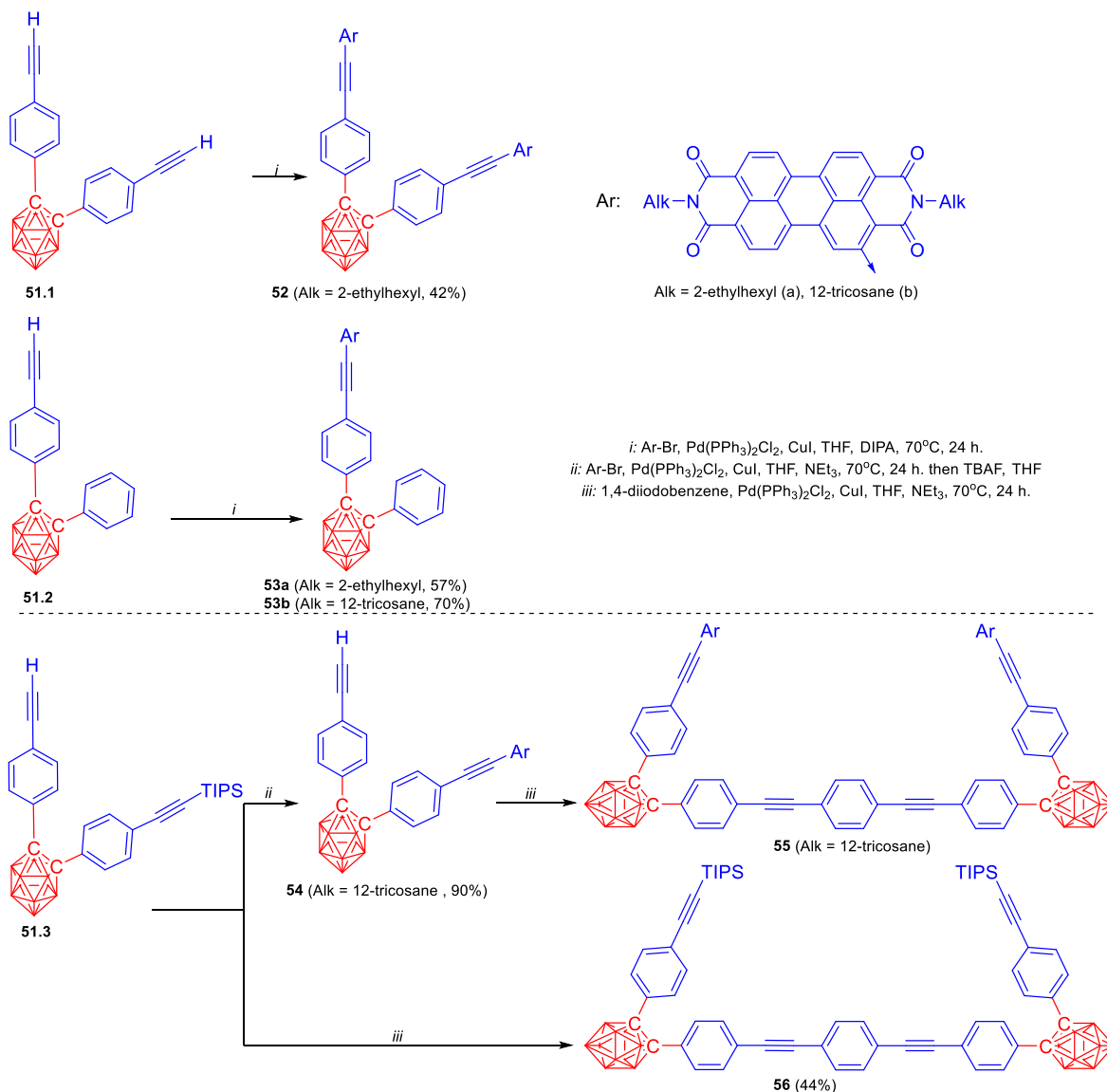
**Scheme 20** Synthesis of *o*-carboranyl derivatives based on PDI.
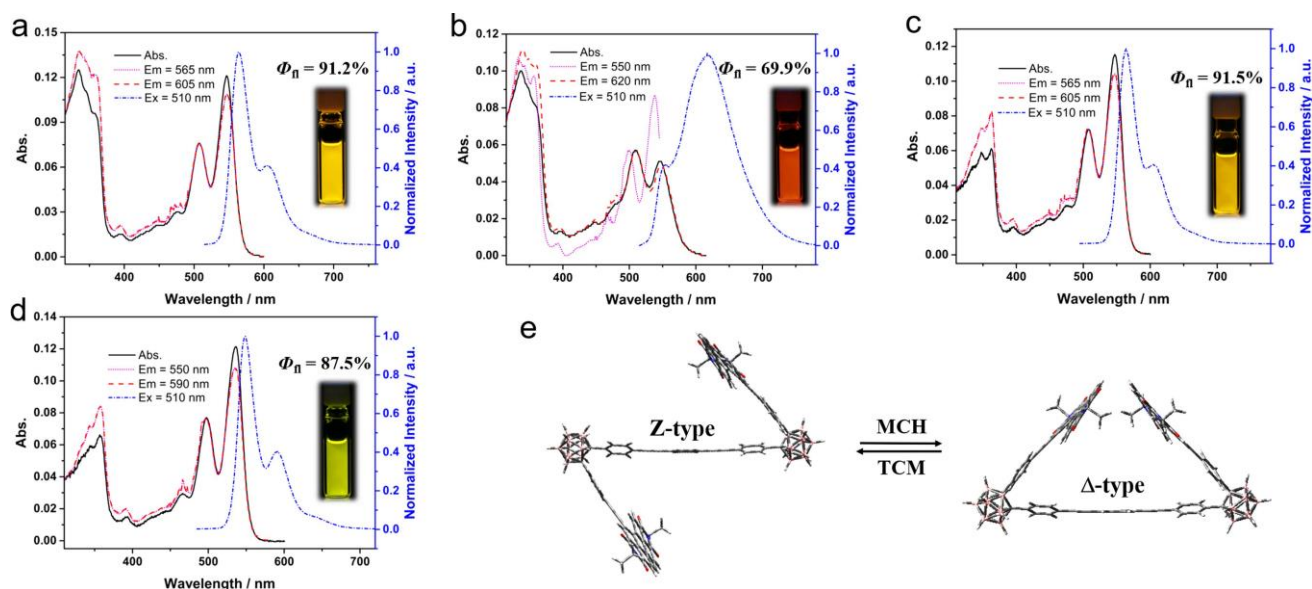
Figure 26 UV-Vis absorption, fluorescence excitation and emission spectra of **55** in CCl$_4$ (TCM) (a) andmethylcyclohexane (MCH) (C = 2.0·10^{-6} mol/L, 298 K) (b); UV-Vis absorption and fluorescence excitation and emission spectra of **53b** in CCl$_4$ (TCM) (c) and methylcyclohexane (MCH) (C = 4.0·10^{-6} mol/L, 298 K) (d); Two optimized ground state structures of **55** (e). Reproduced from Y. Fang and co-workers [77] with permission from the Wiley.
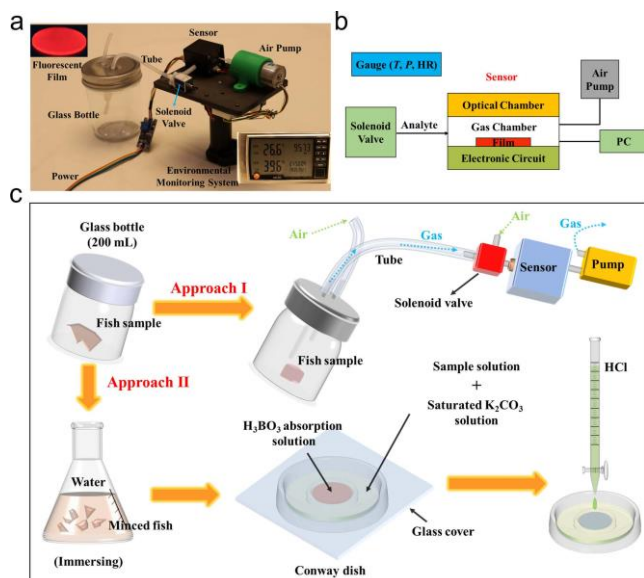

Figure 27 Photos of the home-made sensing platform and the fluorescent film (a); schematic representation of the film sensor (b); comparison of present method with the conventional titration method (c). Reproduced from Y. Fang and co-workers [77] with permission from the Wiley.

In the following work, Yu. Fang et al. [78] developed a chemosensor based on alkenyl substituted *o*-carborane and pyromellitic diimide. The target compound **58** was obtained by Sonogashira cross-coupling with the corresponding dibromoderivative **57** and *o*-carboranyl synthon **51.3** in 56% yield (Scheme 21). The resulting compound was a blue-luminescent fluorophore with absorption in the 350–400 nm range, emission in the 470 nm range, and QY of up to 14% in solvents of different polarity (Figure 28, a). It should be noted that the modification of diimide with *o*-carboranyl led to the appearance of AIE and mechanoluminescent properties in the molecule, the emission intensity in solutions increases up to a tenfold, and the

quantum yield in the solid state and thin films slightly decreased. However, a bathochromic shift of emission up to 500 nm was observed in the thin films (Figure 28, b). The authors developed a device for selective detection of aniline vapor, which is a carcinogen and might also be an early marker of lung cancer. The device was composed of a thin optical system, the working element of which was a thin film of compound **58**. Using a pump, the analyzed gas was fed into the system, and if it contained aniline vapors the luminescence was supposed to be quenched (Figure 28, c). The mechanism was based on the fact that HOMO energy of 56 (–7.55 eV) was lower than that of aniline (–6.37 eV), and in the excited state the photoinduced electron transfer from the HOMO of aniline to **58** occurs, which led to emission quenching.
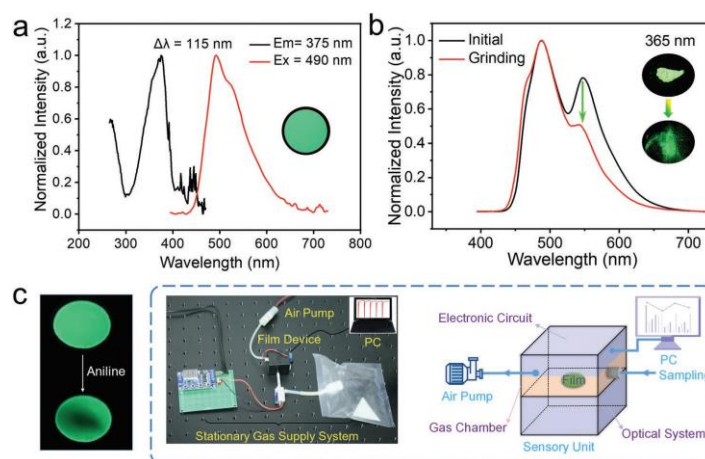
Figure 28 (a) The excitation and fluorescence spectra of **58**-based sensing film. The inset was the fluorescence photo of the **58**-based sensing film; (b) the emission spectra and fluorescence photos of **58** solid in the initial and grinded states; (c) the PL photos of the sensing film before and after fuming with aniline vapor (left). Images of the exploited fluorescence sensing platform and the responding schematic illustration (right). Reproduced from Y. Fang and co-workers [78] with permission from the Wiley.

Dibromoaryl:

57

51.3

Dibromoaryl **57** Pd(Ph₃P)₂Cl₂

CuI, THF, NEt₃

Alk = 2-ethylhexyl

58 (56%)
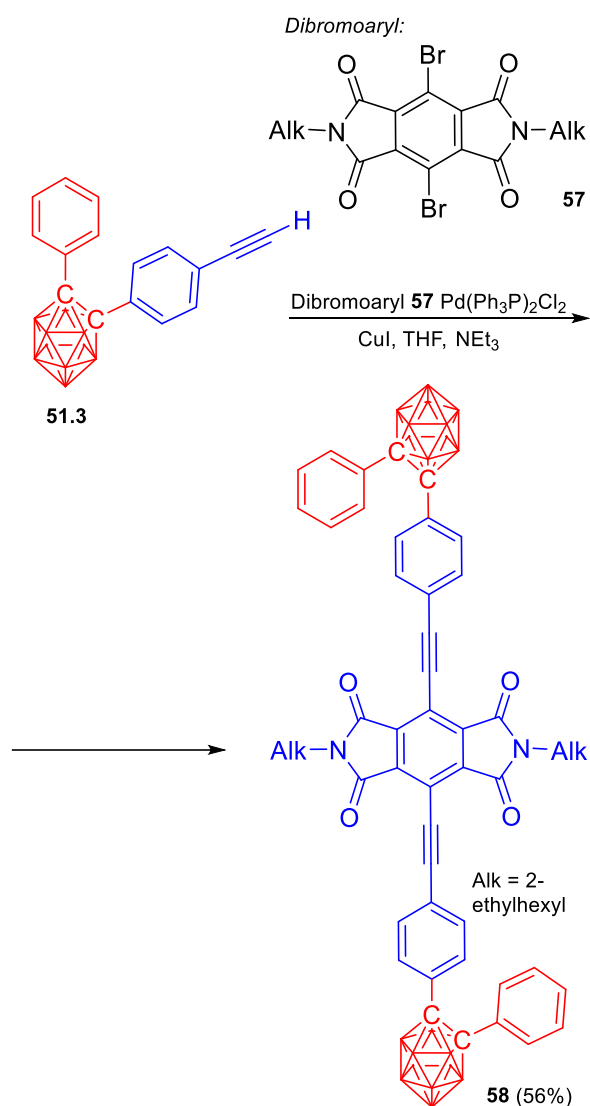
Scheme 21 Synthesis of *o*-carboranyl derivatives based on PMI.

R. Ziessel and A. Harriman synthesized [79] a series of push-pull photoluminescent molecules consisting of fragments of diketopyrrolopyrrole (DPP) and BODIPY, which are EDG and EWG groups separated in space by an *o*-carboranyl spacer **60** (Scheme 22). The method of preparation comprised four stages starting with **37Br** and involving several sequential Sonogashira-type reactions first with the BODIPY fragment and then with DPP (**59.1–59.3**). The emission spectra of this fluorophore exhibited a single broadened peak in the red region (~700 nm), and it was found that the emission intensity decreased with increasing pressure. On the contrary, as the temperature was increased, the emission intensity was found to increase. In both cases, a bathochromic shift of emission was detected, indicating increased planarity along the molecular backbone. The rate constant for energy transfer (k_{EET}) in 60 was $1.9 \cdot 10^{10}$ s⁻¹, which was significantly faster than that of the *p*-carborane-bridged dyad ($k_{EET} = 3.1 \cdot 10^9$ s⁻¹). This phenomenon could be attributed to the shorter separation distance and the specific orientation of the donor and acceptor in the *o*-carborane-bridged dyad. It should be noted that the center-to-center separation between the
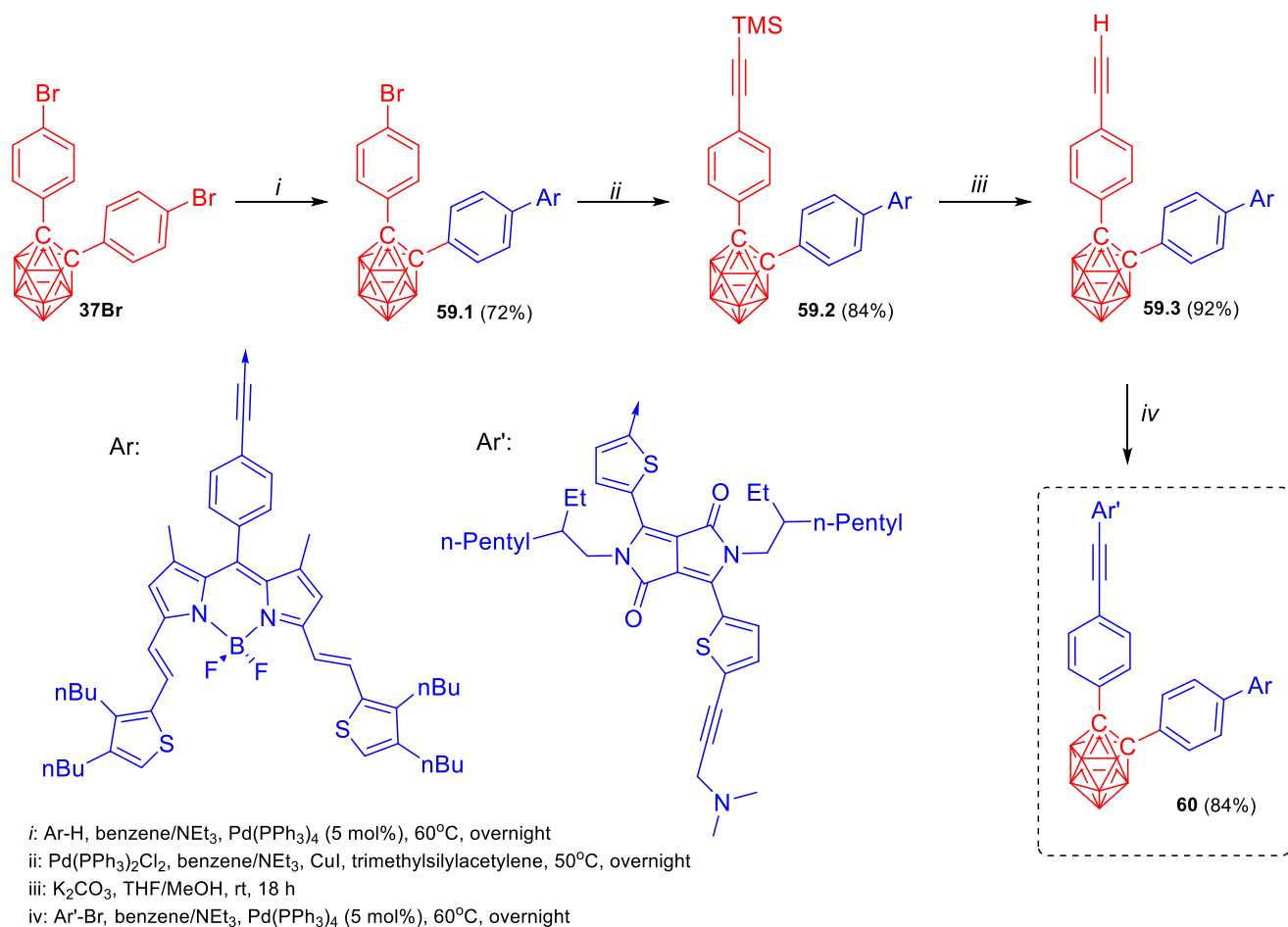
donor and acceptor in **60** is 18.6 Å, which is significantly shorter than the separation in the *p*-carborane-bridged dyad (35.8 Å).

R. Núñez et al. continued their research [80] on the synthesis and investigation of the properties of BODIPY dyes containing an *o*-carboranyl moiety, **63a–b**. The employment of the same *o*-carborane synthon in the Sonogashira reaction with an alkynyl derivative of BODIPY afforded novel fluorophores in 56–81% yields (Scheme 23). The alkynyl π-conjugated system caused a slight hypsochromic shift in the absorption spectra and a consequent increase in the Stokes shift. Additionally, the emission was in the same region of the green light range (520 nm), with quantum yields significantly being reduced to 1% versus 40% in case of the alkenyl analogous compound **12**. Researchers demonstrated the application of these materials for cell bioimaging, but the most significant results were observed for the *m*-carboranyl analog, which was more lipophilic compared to **63a–b**.

Our research group [81] recently developed a preparation method for *o*-carborane-derived luminophores containing a vinylacetylene spacer (Scheme 24). Applying Cu(I)-catalyzed reaction of the corresponding *o*-carboranyl derivative **28** with arylboronic acids, four photoactive molecules **64a-d** were synthesized in 23-55% yields. The obtained compounds possessed absorption in the 300-400 nm region, emission up to 700 nm, and quantum yields of up to 99% in nonpolar solvents (Figure 29). It was found that these systems did not exhibit typical behavior for push-pull systems, and the nature of their emission was related to phosphorescence, which was further verified by TD-DFT calculations. It is worth mentioning that these systems exhibited rigidochromism, but no aggregative and chemosensory properties were found.
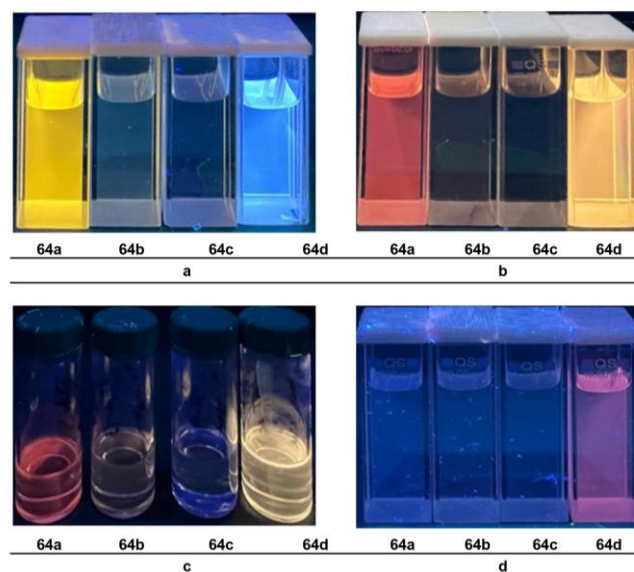
Figure 29 Photos of compounds **64a-d** in solution at room temperature under UV irradiation (λ_{ex} = 365 nm); (a)in cyclohexane with $C = 10^{-5}$ mol/L; (b) in toluene with $C = 10^{-5}$ mol/L; (c) in toluene with $C = 10^{-3}$ mol/L; (d) in 2-methyltetrahydrofuran with $C = 10^{-5}$ mol/L.

i: Ar-H, benzene/NEt$_3$, Pd(PPh$_3$)$_4$ (5 mol%), 60°C, overnight
ii: Pd(PPh$_3$)$_2$Cl$_2$, benzene/NEt$_3$, CuI, trimethylsilylacetylene, 50°C, overnight
iii: K$_2$CO$_3$, THF/MeOH, rt, 18 h
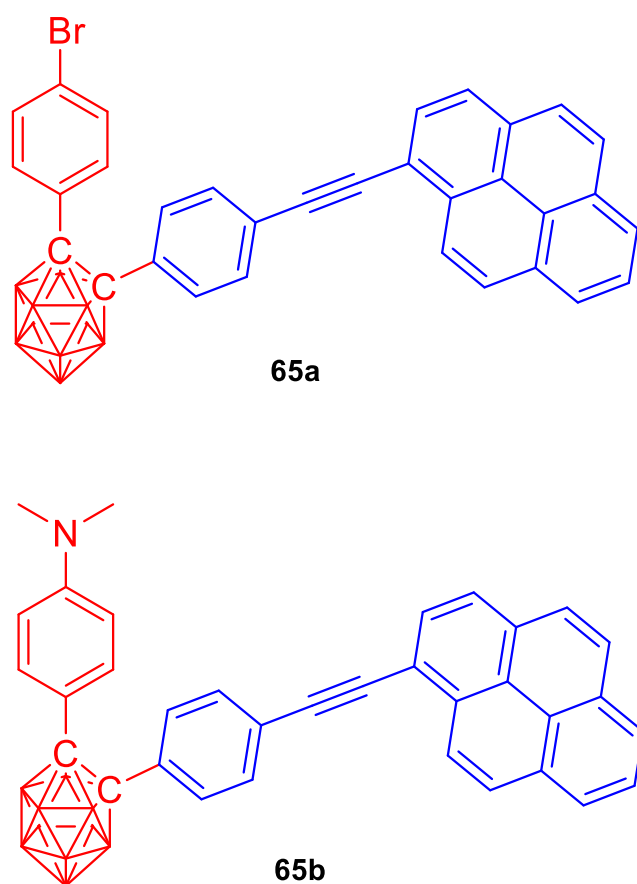iv: Ar'-Br, benzene/NEt$_3$, Pd(PPh$_3$)$_4$ (5 mol%), 60°C, overnight

Scheme 22 Synthesis of three molecular dyads for through-space electronic energy transfer.
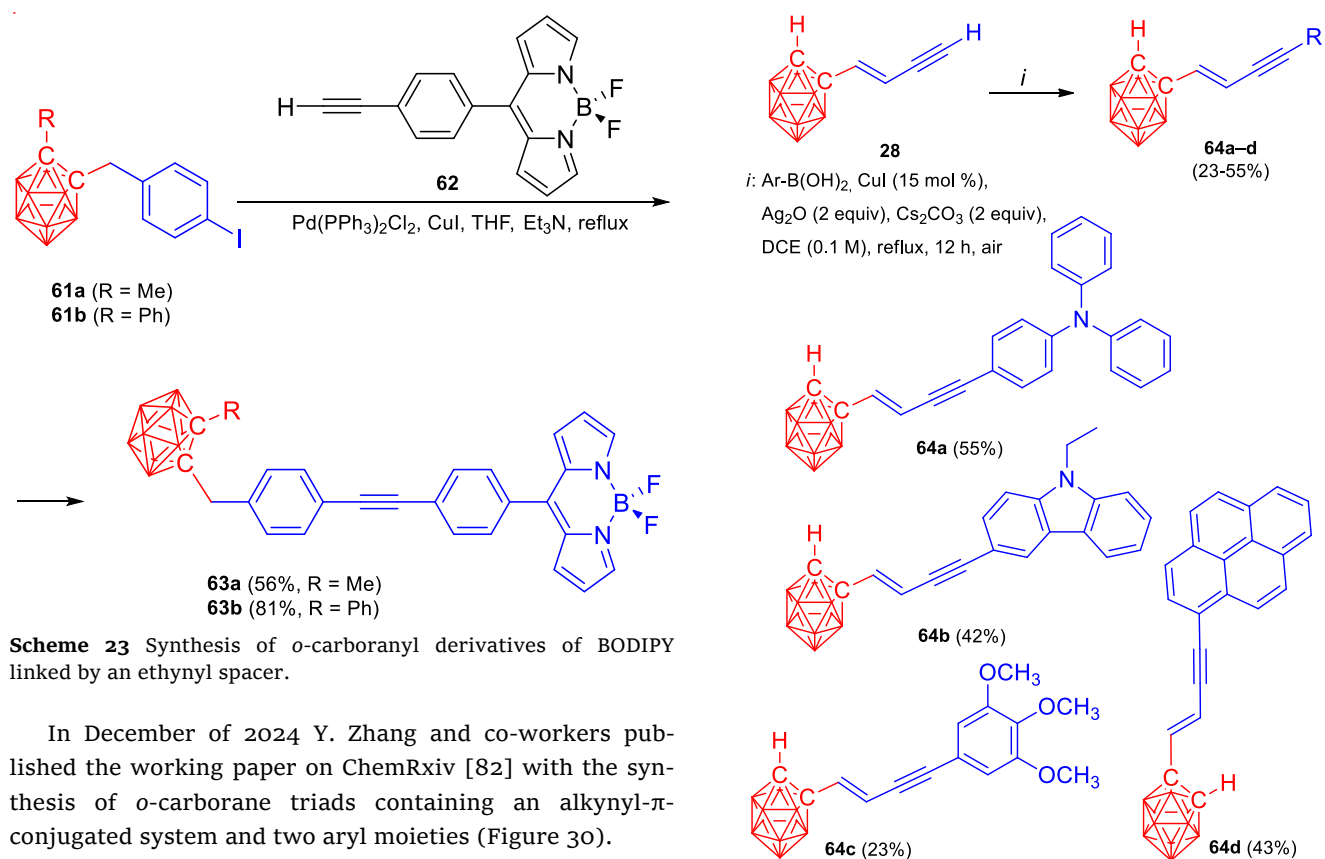
Scheme 23 Synthesis of *o*-carboranyl derivatives of BODIPY linked by an ethynyl spacer.

In December of 2024 Y. Zhang and co-workers published the working paper on ChemRxiv [82] with the synthesis of *o*-carborane triads containing an alkynyl-π-conjugated system and two aryl moieties (Figure 30).

i: Ar-B(OH)$_2$, CuI (15 mol %),
   Ag$_2$O (2 equiv), Cs$_2$CO$_3$ (2 equiv),
   DCE (0.1 M), reflux, 12 h, air

Scheme 24 Synthesis of *o*-carboranyl vinyl acetylene derivatives.

65a

65b

Figure 30 Two *o*-carborane triads containing an alkynyl-π-conjugated system and two aryl moieties.

The authors proposed a three-step synthesis starting with condensation of decaborane (**14**) with tolane-type derivatives, followed by Sonogashira and Buchwald-Harting cross-couplings, resulting in two novel *o*-carborane-derived luminophores **65a–b**. They found that intermolecular charge transfer between pyrene units and *o*-carborane moieties occurred as a result of σ · · · π interactions between these moieties. These compounds exhibited aggregation-induced emission in both solution and solid state. The presence of multiple emitter species made **65a-b** a potential candidate for white light emission and thermally activated delayed fluorescence (TADF).

In this section, the methods of synthesis and photophysical properties of luminophores based on alkynyl π-conjugated systems have been discussed. For their preparation, researchers use two basic synthons, in which the ethynyl fragment is directly bonded to the *o*-carboranyl cluster or *via* a phenyl spacer. The most widely used synthetic technique for the design of this kind of systems is the Sonogashira reaction or the decaborane strategy application.

4. Conclusions and Limitations

Thus, in this review the existing studies on luminophores based on C-substituted *o*-carboranyl clusters bearing an alkenyl or alkynyl conjugation system have been consid-

ered. In the field of synthetic approaches, the synthetic methods of these systems have been shown to be limited by various cross-coupling reactions (Sonogashira, Heck, etc.), or condensation with decaborane.

The most promising in regard to the functional properties are alkynyl derivatives that are directly bonded to the *o*-carborane cluster or via a spacer. These compounds show emission from blue to red region, incorporation of *o*-carborane moieties in most cases leads to aggregation and mechanoluminescent properties. In some cases, the incorporation of o-carboranyl fragments was found to decrease the quantum yield caused by the active rotation of *o*-carborane, leading to a higher number of non-radiative transitions. By incorporation of spacers between the aryl and *o*-carboranyl substituents, a tuneable change in the emission mechanism from intramolecular charge transfer to excimer emission can be achieved. These photoactive systems can be employed as organic semiconductor materials, transistors, switches, chemosensors, components of organic light-emitting diodes, and may also be applied in photodynamic therapy. On the other hand, less explored are alkenyl luminescent systems, on the basis of which molecular electronics devices have not yet been developed so far. Nevertheless, the incorporation of *o*-carboranyl moieties result in aggregation properties, phosphorescence and long-wavelength emission. The modification of *o*-carborane with bulk substituents on the second carbon atom seems to contribute to the decreasing of intramolecular rotation and to the enhancement of photophysical properties.

Subsequently, the following ways for the further development of photoactive systems are the elaboration of new synthetic approaches and expansion of possibilities of using quantum chemistry and modeling methods for the directed design of conjugated systems with technologically relevant properties.

Author contributions

Conceptualization: O.N.C., V.N.C.
Funding acquisition: T.D.M.
Investigation: T.D.M., T.A.I.
Supervision: V.N.C., M.V.V.
Writing – original draft: T.D.M., T.A.I.
Writing – review & editing: M.V.V.

Conflict of interest

The authors declare no conflict of interest.

Additional information

Timofey D. Moseev. PhD in Chemistry, Associate Professor at the Research, Education and Innovation Center of Chemical and Pharmaceutical Technologies of the Institute of Chemical Engineering.
Research interests: *o*-carborane, C-H functionalization, green chemistry, organofluorine compounds, fluorophores, organic electronics.
Scopus AD 57196048249

Tair A. Idrisov. PhD student, Research Engineer at the Research, Education and Innovation Center of Chemical and Pharmaceutical Technologies of the Institute of Chemical Engineering.
Research interests: organic derivatives of *o*-carborane, C-H functionalization, cross-coupling reactions, *o*-carborane cluster luminophores.
Scopus AD 58854637800

Mikhail V. Varaksin. Doctor of Chemical Sciences, Professor of the Department of Organic and Biomolecular Chemistry of the Institute of Chemical Engineering; Professor of the Laboratory of Coordination Compounds, I.Ya. Postovsky Institute of Organic Synthesis, Ural Branch of the Russian Academy of Sciences.
Research interests: C-H functionalization, green chemistry, heterocyclic compounds, functional materials, organic electronics, medicinal chemistry.
Scopus AD 26637829900

Valery N. Charushin. Academician of the Russian Academy of Sciences, Doctor of Chemical Sciences, Professor of the Department of Organic and Biomolecular Chemistry of the Institute of Chemical Engineering; Chief Researcher of I.Ya. Postovsky Institute of Organic Synthesis, Ural Branch of the Russian Academy of Sciences.
Research interests: non-metallic C-H functionalization of (het)arenes, PASE-methods in the synthesis of azaheterocycles, biologically active compounds, medicinal chemistry, luminophores.
Scopus AD 7006350819

Oleg N. Chupakhin. Academician of the Russian Academy of Sciences, Doctor of Chemical Sciences, Professor of the Department of Organic and Biomolecular Chemistry of the Institute of Chemical Engineering; Head of the Laboratory of Coordination Compounds of I.Ya. Postovsky Institute of Organic Synthesis, Ural Branch of the Russian Academy of Sciences.
Research interests: nucleophilic substitution of hydrogen, non-metal-catalyzed C-H functionalization of (het)arenes, one-step regioselective methods for construction of complex heterocyclic structures, chemistry of fluorine-containing compounds, chemical aspects of environmental protection, biologically active compounds, medicinal chemistry.
Scopus AD 7006259116

References

1. Grimes RN. 2016. Carboranes. 3rd ed. San Diego, CA: Academic Press.
2. Crabtree R, Mingos M, Eds., Comprehensive Organometallic Chemistry III. London, England: Elsevier Science, 2006.
3. Poater J, Solà M, Viñas C, Teixidor F. A aromaticity and three-dimensional aromaticity: Two sides of the same coin? Angew Chem Int Ed Engl. 2014;53(45):12191–12195. doi:10.1002/anie.201407359
4. Poater J, Viñas C, Bennour I, Escayola S, Solà M, Teixidor F. Too persistent to give up: Aromaticity in boron clusters survives radical structural changes. J Am Chem Soc. 2020;142(20):9396–9407. doi:10.1021/jacs.0c02228
5. Olah GA, Wade K, Williams RE. 1991. Electron deficient boron and carbon clusters. Nashville, TN: John Wiley & Sons.
6. Qiu Z. Recent advances in transition metal-mediated functionalization of o-carboranes. Tetrahedron Lett. 2015;56(8):963–971. doi:10.1016/j.tetlet.2015.01.038
7. Dong B, Oyelade A, Kelber JA. Carborane-based polymers: a novel class of semiconductors with tunable properties. Phys Chem Chem Phys. 2017;19(18):10986–10997. doi:10.1039/c7cp00835j
8. Zhang X, Rendina LM, Müllner M. Carborane-containing polymers: Synthesis, properties, and applications. ACS Polym Au. 2024;4(1):7–33. doi:10.1021/acspolymersau.3c00030
9. Marfavi A, Kavianpour P, Rendina LM. Carboranes in drug discovery, chemical biology and molecular imaging. Nat Rev Chem. 2022;6(7):486–504. doi:10.1038/s41570-022-00400-x
10. Fox M. Cage C-H···X interactions in solid-state structures of icosahedral carboranes. Coord Chem Rev. 2004;248(5–6):457–476. doi:10.1016/j.ccr.2003.10.002
11. Liu X-R, Cui P-F, García-Rodeja Y, Solà M, Jin G-X. Formation and reactivity of a unique M···C-H interaction stabilized by carborane cages. Chem Sci. 2024;15(24):9274–9280. doi:10.1039/d4sc01158a
12. Prasanth D, Sunitha DV, Kumar PR, Darshan GP. Design strategies, luminescence mechanisms, and solid-state lighting applications of lanthanide-doped phosphorescent materials. ChemPhysMater. 2024;9:4. doi:10.1016/j.chphma.2024.09.004
13. Wang T, Su X, Zhang Xuepeng, Huang W, Huang L, Zhang Xingyuan, Sun X, Luo Y, Zhang G. A combinatory approach towards the design of organic polymer luminescent materials. J Mater Chem C Mater Opt Electron Devices. 2019;7(32):9917–9925. doi:10.1039/c9tc02266j
14. Achelle S, Rodríguez-López J, Guen FR-L. Photoluminescence properties of aryl-, arylvinyl-, and arylethynylpyrimidine derivatives. ChemistrySelect. 2018;3(6):1852–1886. doi:10.1002/slct.201702472
15. Raheem AA, Praveen C. π-Distorted charge transfer chromophores and their materials chemistry in organic photovoltaics. J Mater Chem C Mater Opt Electron Devices. 2024;12(24):8611–8646. doi:10.1039/d4tc01424c
16. Meng Y, Lin X, Huang J, Zhang L. Recent advances in carborane-based crystalline porous materials. Molecules. 2024;29(16):3916. doi:10.3390/molecules29163916
17. Kim S, Lee JH, So H, Ryu J, Lee J, Hwang H, Kim Y, Park MH, Lee KM. Spirobifluorene-based o-carboranyl compounds: Insights into the rotational effect of carborane cages on photoluminescence. Chem. 2020;26(2):548–557. doi:10.1002/chem.201904491
18. Wang H. Recent advances on carborane-based ligands in low-valent group 13 and group 14 elements chemistry. Chin Chem Lett. 2022;33(8):3672–3680. doi:10.1016/j.cclet.2021.12.016
19. Pigot C, Noirbent G, Brunel D, Dumur F. Recent advances on push–pull organic dyes as visible light photoinitiators of polymerization. Eur Polym J. 2020;133(109797):109797. doi:10.1016/j.eurpolymj.2020.109797
20. Pal A, Karmakar M, Bhatta SR, Thakur A. A detailed insight into anion sensing based on intramolecular charge transfer (ICT) mechanism: A comprehensive review of the years 2016

to 2021. Coord Chem Rev. 2021;448(214167):214167. doi:10.1016/j.ccr.2021.214167

21. Kato S-I, Diederich F. Non-planar push-pull chromophores. Chem Commun (Camb). 2010;46(12):1994–2006. doi:10.1039/b926601a

22. Raghava T, Banerjee S. Amino-terephthalonitrile and amino-terephthalate-based single benzene fluorophores - compact color tunable molecular dyes for bioimaging and bioanalysis. Chem Asian J. 2024;19(23):e202400898. doi:10.1002/asia.202400898

23. Rammohan A, Mallikarjuna Reddy G, Khasanov AF, Chalapathi U, Santra S, Zyryanov GV, Park S-H. Aurone synthesis and fluorescence properties for chemosensory, optoelectronic and biological applications: A review. Dyes Pigm. 2024;223(111967):111967. doi:10.1016/j.dyepig.2024.111967

24. Verbitskiy EV, Lipunova GN, Nosova EV, Charushin VN. 2023. Advances in the design of functionalized 1,4-diazines as components for photo- or/and electroactive materials. Dyes Pigm. 2023;220(111763):111763. doi:10.1016/j.dyepig.2023.111763

25. Lavrinchenko IA, Moseev TD, Varaksin MV, Charushin VN, Chupakhin ON. Luminophores based on 2H-1,2,3-triazoles: synthesis, photophysical properties, and application prospects. Russ Chem Rev. 2024;93(10):RCR5130. doi:10.59761/rcr5130

26. Lipunova GN, Nosova EV, Zyryanov GV, Charushin VN, Chupakhin ON. 1,2,4,5-Tetrazine derivatives as components and precursors of photo- and electroactive materials. Org Chem Front. 2021;8(18):5182–5205. doi:10.1039/d1qo00465d

27. Nosova EV, Lipunova GN, Zyryanov GV, Charushin VN, Chupakhin ON. Functionalized 1,3,5-triazine derivatives as components for photo- and electroluminescent materials. Org Chem Front. 2022;9(23):6646–6683. doi:10.1039/d2qo00961g

28. Ordóñez-Hernández J, Planas JG, Núñez R. Carborane-based BODIPY dyes: synthesis, structural analysis, photophysics and applications. Front Chem. 2024;12:1485301. doi:10.3389/fchem.2024.1485301

29. Ran Z, Zhao W, Shi J, Ji L. 2025. Luminescent o-carboranyl-containing molecules: A promising platform for stimuli-responsive smart materials. Dyes Pigm. 232(112484):112484. doi:10.1016/j.dyepig.2024.112484.

30. Tanaka K, Gon M, Ito S, Ochi J, Chujo Y. Recent progresses in the mechanistic studies of aggregation-induced emission-active boron complexes and clusters. Coord Chem Rev. 2022;472(214779):214779. doi:10.1016/j.ccr.2022.214779

31. Mukherjee S, Thilagar P. Boron clusters in luminescent materials. Chem Commun (Camb). 2016;52(6):1070–1093. doi:10.1039/c5cc08213g

32. Núñez R, Tarrés M, Ferrer-Ugalde A, de Biani FF, Teixidor F. Electrochemistry and photoluminescence of icosahedral carboranes, boranes, metallacarboranes, and their derivatives. Chem Rev. 2016;116(23):14307–14378. doi:10.1021/acs.chemrev.6b00198

33. Ochi J, Tanaka K, Chujo Y. Recent progress in the development of solid-state luminescent o-carboranes with stimuli responsivity. Angew Chem Int Ed Engl. 2020;59(25):9841–9855. doi:10.1002/anie.201916666

34. Smyshliaeva LA, Varaksin MV, Charushin VN, Chupakhin ON. Azaheterocyclic derivatives of ortho-carborane: Synthetic strategies and application opportunities. Synthesis (Mass). 2020;52(03):337–352. doi:10.1055/s-0039-1690733

35. Zhao D, Xie Z. Recent advances in the chemistry of carborynes. Coord Chem Rev. 2016;314:14–33. doi:10.1016/j.ccr.2015.07.011

36. Gon M, Tanaka K, Chujo Y. 2019. Concept of excitation-driven boron complexes and their applications for functional luminescent materials. Bull Chem Soc Jpn. 2019;92(1):7–18. doi:10.1246/bcsj.20180245

37. Ferrer-Ugalde A, Juárez-Pérez EJ, Teixidor F, Viñas C, Sillanpää R, Pérez-Inestrosa E, Núñez R. Synthesis and characterization of new fluorescent styrene-containing carborane de-

rivatives: the singular quenching role of a phenyl substituent. Chem. 2012;18(2):544–553. doi:10.1002/chem.201101881

38. Cabrera-González J, Viñas C, Haukka M, Bhattacharyya S, Gierschner J, Núñez R. Photoluminescence in carborane-stilbene triads: A structural, spectroscopic, and computational study. Chem. 2016;22(38):13588–13598. doi:10.1002/chem.201601177

39. Ferrer-Ugalde A, Cabrera-González J, Juárez-Pérez EJ, Teixidor F, Pérez-Inestrosa E, Montenegro JM, Sillanpää R, Haukka M, Núñez R. Carborane-stilbene dyads: the influence of substituents and cluster isomers on photoluminescence properties. Dalton Trans. 2017;46(7):2091–2104. doi:10.1039/c6dt04003a

40. Cabrera-González J, Bhattacharyya S, Milián-Medina B, Teixidor F, Farfán N, Arcos-Ramos R, Vargas-Reyes V, Gierschner J, Núñez R. Tetrakis[(p - dodecacarboranyl)methyl]stilbenylethylene: A luminescent tetraphenylethylene (TPE) core system: Tetrakis[(p-dodecacarboranyl)methyl]stilbenylethylene: A luminescent tetraphenylethylene (TPE) core system. Eur J Inorg Chem. 2017;38–39:4575–4580. doi:10.1002/ejic.201700453

41. Chaari M, Cabrera-González J, Kelemen Z, Viñas C, Ferrer-Ugalde A, Choquesillo-Lazarte D, Ben Salah A, Teixidor F, Núñez R. Luminescence properties of carborane-containing distyrylaromatic systems. J Organomet Chem. 2018;865:206–213. doi:10.1016/j.jorganchem.2018.03.002

42. Becerra-González JG, Peña-Cabrera E, Belmonte-Vázquez JL. From blue to red. Reaching the full visible spectrum with a single fluorophore: BODIPY. Tetrahedron. 2024;168(134334):134334. doi:10.1016/j.tet.2024.134334

43. Prandi C, Núñez R, Bellomo C, Blangetti M, Deagostino A, Lombardi C, Viñas C, Cabrera-González J, Chaari M, Nerea Gaztelumendi N, et al. Carborane-BODIPY dyads: New photoluminescent materials through an efficient Heck coupling. Chem. 2018. doi:10.1002/chem.201802901

44. Bellomo C, Zanetti D, Cardano F, Sinha S, Chaari M, Fin A, Maranzana A, Núñez R, Blangetti M, Prandi C. 2021. Red light-emitting Carborane-BODIPY dyes: Synthesis and properties of visible-light tuned fluorophores with enhanced boron content. Dyes Pigm. 2021;194(109644):109644. doi:10.1016/j.dyepig.2021.109644

45. Nar I, Atsay A, Buyruk A, Pekbelgin Karaoğlu H, Burat AK, Hamuryudan E. BODIPY–ortho-carborane–tetraphenylethylene triad: synthesis, characterization, and properties. New J Chem. 2019;43(11):4471–4476. doi:10.1039/c9nj00177h

46. Cabrera-González J, Ferrer-Ugalde A, Bhattacharyya S, Chaari M, Teixidor F, Gierschner J, Núñez R. Fluorescent carborane–vinylstilbene functionalised octasilsesquioxanes: synthesis, structural, thermal and photophysical properties. J Mater Chem C Mater Opt Electron Devices. 2017;5(39):10211–10219. doi:10.1039/c7tc03319b

47. Xie L-H, Yang S-H, Lin J-Y, Yi M-D, Huang W. Fluorene-based macromolecular nanostructures and nanomaterials for organic (opto)electronics. Philos Trans A Math Phys Eng Sci. 2013;371(2000):20120337. doi:10.1098/rsta.2012.0337

48. Ferrer-Ugalde A, González-Campo A, Viñas C, Rodríguez-Romero J, Santillan R, Farfán N, Sillanpää R, Sousa-Pedrares A, Núñez R, Teixidor F. Fluorescence of new o-carborane compounds with different fluorophores: can it be tuned? Chem. 2014;20(32):9940–9951. doi:10.1002/chem.201402396

49. Zhu L, Lv W, Liu S, Yan H, Zhao Q, Huang W. Carborane enhanced two-photon absorption of tribranched fluorophores for fluorescence microscopy imaging. Chem Commun (Camb). 2013;49(90):10638–10640. doi:10.1039/c3cc46276e

50. Smyshliaeva LA, Varaksin MV, Fomina EI, Joy MN, Bakulev VA, Charushin VN, Chupakhin ON. Cu(I)-catalyzed cycloaddition of vinylacetylene ortho-carborane and arylazides in the design of 1,2,3-triazolyl-modified vinylcarborane fluorophores. Organometallics. 2020;39(20):3679–3688. doi:10.1021/acs.organomet.0c00478

51. Guo J, Liu D, Zhang Jiahui, Zhang Jiji, Miao Q, Xie Z. o-Carborane functionalized pentacenes: synthesis, molecular packing and ambipolar organic thin-film transistors. Chem Commun (Camb). 2015;51(60):12004–12007. doi:10.1039/c5cc03608a

52. Wu X, Guo J, Quan Y, Jia W, Jia D, Chen Y, Xie Z. Cage carbon-substitute does matter for aggregation-induced emission features of o-carborane-functionalized anthracene triads. J Mater Chem C Mater Opt Electron Devices. 2018;6(15):4140–4149. doi:10.1039/c8tc00380g

53. Yuhara K, Tanaka K. Direction switching and self-recovering mechanochromic luminescence of anthracene-modified o-carboranes. Chem. 2023;29(44). doi:10.1002/chem.202301189

54. Nishino K, Yamamoto H, Tanaka K, Chujo Y. Solid-state thermochromic luminescence through twisted intramolecular charge transfer and excimer formation of a Carborane–Pyrene dyad with an ethynyl spacer. Asian J Org Chem. 2017;6(12):1818–1822. doi:10.1002/ajoc.201700390

55. Nishino K, Yamamoto H, Ochi J, Tanaka K, Chujo Y. Time-dependent emission enhancement of the ethynylpyrene-o-carborane dyad and its application as a luminescent color sensor for evaluating water contents in organic solvents. Chem Asian J. 2019;14(9):1577–1581. doi:10.1002/asia.201900396

56. Yamamoto H, Ochi J, Yuhara K, Tanaka K, Chujo Y. Switching between intramolecular charge transfer and excimer emissions in solids based on aryl-modified ethynyl–o-carboranes. Cell Rep Phys Sci. 2022;3(2):100758. doi:10.1016/j.xcrp.2022.100758

57. Ochi J, Tanaka K, Chujo Y. Dimerization-induced solid-state excimer emission showing consecutive thermochromic luminescence based on acridine-modified o-carboranes. Inorg Chem. 2021;60(12):8990–8997. doi:10.1021/acs.inorgchem.1c00901

58. Ochi J, Tanaka K, Chujo Y. Improvement of solid-state excimer emission of the aryl-ethynyl-o -carborane skeleton by acridine introduction: Improvement of solid-state excimer emission of the aryl-ethynyl-o -carborane skeleton by acridine introduction. Eur J Org Chem. 2019;19:2984–2988. doi:10.1002/ejoc.201900212

59. Jin GF, Cho Y-J, Wee K-R, Hong SA, Suh I-H, Son H-J, Lee J-D, Han W-S, Cho DW, Kang SO. BODIPY functionalized o-carborane dyads for low-energy photosensitization. Dalton Trans. 2015;44(6):2780–2787. doi:10.1039/c4dt03123g

60. Kokado K, Tokoro Y, Chujo Y. 2009. Luminescent and axially chiral π-conjugated polymers linked by carboranes in the main chain. Macromolecules. 2009;42(23):9238–9242. doi:10.1021/ma902094u

61. Kokado K, Chujo Y. Emission via aggregation of alternating polymers with o-carborane and p-Phenylene–Ethynylene sequences. Macromolecules. 2009;42(5):1418–1420. doi:10.1021/ma8027358

62. Kokado K, Chujo Y. Polymer reaction of poly(p-phenylene–ethynylene) by addition of decaborane: modulation of luminescence and heat resistance. Polym J. 2010;42(5):363–367. doi:10.1038/pj.2010.13

63. Kokado K, Tominaga M, Chujo Y. Aromatic ring-fused carborane-based luminescent π-conjugated polymers. Macromol Rapid Commun. 2010;31(15):1389–1394. doi:10.1002/marc.201000160

64. Kokado K, Nagai A, Chujo Y. Energy transfer from aggregation-induced emissive o-carborane. Tetrahedron Lett. 2011;52(2):293–296. doi:10.1016/j.tetlet.2010.11.026

65. Kokado K, Chujo Y. Multicolor tuning of aggregation-induced emission through substituent variation of diphenyl-o-carborane. J Org Chem. 2011;76(1):316–319. doi:10.1021/jo101999b

66. Fang W, Liu K, Wang G, Liang Y, Huang R, Liu T, Ding L, Peng J, Peng H, Fang Y. Dual-phase emission AIEgen with ICT properties for VOC chromic sensing. Anal Chem. 2021;93(24):8501–8507. doi:10.1021/acs.analchem.1c00980

67. Bureš F. Fundamental aspects of property tuning in push–pull molecules. RSC Adv. 2014;4(102):58826–58851. doi:10.1039/c4ra11264d

68. Son MR, Cho Y-J, Kim S-Y, Son H-J, Cho DW, Kang SO. Direct observation of the photoinduced electron transfer processes of bis(4-arylphenylamino benzo)-ortho-carborane using transient absorption spectroscopic measurements. Phys Chem Chem Phys. 2017;19(36):24485–24492. doi:10.1039/c7cp04505k

69. Wang Z, Jiang P, Wang T, Moxey GJ, Cifuentes MP, Zhang C, Humphrey MG. Blue-shifted emission and enhanced quantum efficiency viaπ-bridge elongation in carbazole-carborane dyads. Phys Chem Chem Phys. 2016;18(23):15719–15726. doi:10.1039/c6cp02870e

70. Kokado K, Chujo Y.. A luminescent coordination polymer based on bisterpyridyl ligand containing o-carborane: two tunable emission modes. Dalton Trans. 2011;40(9):1919–1923. doi:10.1039/c1dt90011k

71. Nishino K, Uemura K, Tanaka K, Chujo Y. Dual emission via remote control of molecular rotation of o-carborane in the excited state by the distant substituents in tolane-modified dyads. New J Chem. 2018;42(6):4210–4214. doi:10.1039/c7nj04283c

72. Wada K, Hashimoto K, Ochi J, Tanaka K, Chujo Y. Rational design for thermochromic luminescence in amorphous polystyrene films with bis-o-carborane-substituted enhanced conjugated molecule having aggregation-induced luminochromism. Aggregate (Hoboken). 2021;2(5). doi:10.1002/agt2.93

73. Mori H, Nishino K, Wada K, Morisaki Y, Tanaka K, Chujo Y. Modulation of luminescence chromic behaviors and environment-responsive intensity changes by substituents in bis-o-carborane-substituted conjugated molecules. Mater Chem Front. 2018;2(3):573–579. doi:10.1039/c7qm00486a

74. Liang S, Jiang X, Xiao C, Li C, Chen Q, Li W. Double-cable conjugated polymers with pendant rylene diimides for single-component organic solar cells. Acc Chem Res. 2021;54(9):2227–2237. doi:10.1021/acs.accounts.1c00070

75. Zhan X, Facchetti A, Barlow S, Marks TJ, Ratner MA, Wasielewski MR, Marder SR. Rylene and related diimides for organic electronics. Adv Mater. 2011;23(2):268–284. doi:10.1002/adma.201001402

76. Shang C, Wang G, Wei Y-C, Jiang Q, Liu K, Zhang M, Chen Y-Y, Chang X, Liu F, Yin S, et al. Excimer formation of perylene bisimide dyes within stacking-restrained folda-dimers: Insight into anomalous temperature responsive dual fluorescence. CCS Chem. 2022;4(6):1949–1960. doi:10.31635/ccschem.021.202100871

77. Jiang Q, Wang Z, Wang G, Liu K, Xu W, Shang C, Gou X, Liu T, Fang Y. A configurationally tunable perylene bisimide derivative-based fluorescent film sensor for the reliable detection of volatile basic nitrogen towards fish freshness evaluation. Chin J Chem. 2022;40(2):201–208. doi:10.1002/cjoc.202100626

78. Gao X, Huang R, Fang W, Huang W, Yin Z, Liu Y, Huang X, Ding L, Peng H, Fang Y. A portable fluorescence sensor with improved performance for aniline monitoring. Adv Mater Interfaces. 2022;9(34):2201275. doi:10.1002/admi.202201275

79. Harriman A, Alamiry MAH, Hagon JP, Hablot D, Ziessel R. Through-space electronic energy transfer across proximal molecular dyads. Angew Chem Int Ed Engl. 2013;52(26):6611–6615. doi:10.1002/anie.201302081

80. Labra-Vázquez P, Flores-Cruz R, Galindo-Hernández A, Cabrera-González J, Guzmán-Cedillo C, Jiménez-Sánchez A, Lacroix PG, Santillan R, Farfán N, Núñez R. Tuning the cell uptake and subcellular distribution in BODIPY-carboranyl dyads: An experimental and theoretical study. Chemistry. 2020;26(69):16530–16540. doi:10.1002/chem.202002600

81. Moseev TD, Idrisov TA, Varaksin MV, Tsmokaluk AN, Charushin VN, Chupakhin ON. Copper-catalyzed Sonogashira-type coupling reaction of vinylacetylene ortho-carborane with boronic acid in the synthesis of luminophores with

phosphorescent emission. Reactions. 2024;5(4):868–882. doi:10.3390/reactions5040046

82. Zhang Y, Lalancette R, Galoppini E. Properties of o-carborane triads: Non-covalent σ...π interactions and intermolecular charge transfer. ChemRxiv. 2024. doi:10.26434/chemrxiv-2024-t6khm